Received: 24 March 2025 | Accepted: 7 January 2026

DOI: 10.1111/1365-2745.70305

BRITISH ECOLOGICAL SOCIETY Journal of Ecology

RESEARCH ARTICLE

Unravelling the drivers of island species richness in tropical savannas

Henrique A. Mews[1] | Denis S. Nogueira[2] | Ben Hur Marimon-Junior[3] | Reginaldo Constantino[4] | Oliver L. Phillips[5] | Beatriz S. Marimon[3]

[1]Instituto de Ciências Exatas e Naturais, Universidade Federal de Rondonópolis, Rondonópolis, MT, Brazil

[2]Instituto Federal de Mato Grosso, Campus de Primavera do Leste, Primavera do Leste, MT, Brazil

[3]Programa de Pós-Graduação em Ecologia e Conservação, Universidade do Estado de Mato Grosso, Nova Xavantina, MT, Brazil

[4]Departamento de Zoologia, Universidade de Brasília, Brasília, DF, Brazil

[5]School of Geography, Faculty of Environment, University of Leeds, Leeds, UK

Correspondence
Henrique A. Mews
Email: henrique.mews@ufr.edu.br

Funding information
ERC Advanced Grant; Fundação de Amparo à Pesquisa do Estado de Mato Grosso, Grant/Award Number: 97/04; Program of Academic Agreement/Coordination for the Improvement of Higher-Level Education, Grant/Award Number: 109/2007; Brazilian National Council for Scientific and Technological Development (CNPq)—Special Visiting Researcher, Grant/Award Number: 401279/2014-6; Brazilian National Council for Scientific and Technological Development (CNPq)—Research Productivity Grant, Grant/Award Number: 301153/2018-3, 303492/2022-8 and 311027/2019-9; Royal Society Wolfson Research Merit Award

Handling Editor: Charlotte Ndiribe

Abstract

1. Despite their ecological and conservation significance and potential to enrich our understanding of species and habitat dynamics, natural island habitats in seasonal tropical terrestrial environments remain poorly studied. In particular, the mechanisms regulating species diversity in these systems are largely unresolved.
2. We examined how island area, geographic isolation and habitat heterogeneity and availability influence species richness in *campos de murundus*—'fields of earth mounds'—a distinctive ecosystem of South American tropical savannas. We analysed three key biological groups that structure these systems (trees, herbs and termites) using a comprehensive inventory of 373 murundu islands sampled within 11 1-ha plots across the extensive seasonal floodplains of east-central Brazil.
3. Bayesian mixed-effects models showed that tree and herb richness increased with murundu island area, consistent with predictions from island biogeography. Geographic isolation and environmental heterogeneity had no detectable effects at the island scale. Termite richness showed weak relationships with the predictors and no clear association with area or isolation. Island area explained most variation in plant richness, whereas termite assemblages were mainly associated with spatial eigenvectors at intermediate and fine spatial scales. At the landscape scale, tree alpha diversity increased with total abundance and gamma diversity and decreased with beta diversity, suggesting nested assemblages towards larger islands.
4. These results indicate that plant richness in hyperseasonal savannas is driven primarily by murundu island area and local habitat amount, with little evidence for dispersal limitation or strong environmental filtering. Landscape patterns suggest metacommunity dynamics linked to habitat configuration and long-term ecosystem engineering processes involved in murundu formation. In contrast, termite communities appear only weakly structured by the predictors considered.
5. *Synthesis*. Murundu island area explains a substantial proportion of the variation in tree and herb richness, consistent with Island Biogeography Theory. On

average, a 10% increase in island size corresponds to increases of seven tree species and 7.8 herb species. Termite diversity responds weakly to area and isolation, suggesting stronger roles for dispersal constraints, nest-site availability and species interactions. Landscape structure influences plant but not termite diversity.

KEYWORDS
alpha beta and gamma diversity, earth-mound community assembly, Habitat Amount Hypothesis, hyperseasonal savanna, Island Biogeography Theory, landscape–metacommunity interactions, species–area relationships

1 | INTRODUCTION

It is a truth widely acknowledged in ecology that larger areas support more species (Arrhenius, 1921; Dengler, 2009). The species–area relationship applies to many groups of organisms, both in isolated continental habitats (e.g. mountaintops, lakes and vegetation fragments) and in oceanic and fluvial islands (e.g. Fahrig, 2003; Lomolino & Weiser, 2001). In island systems, declines in species richness with increasing geographic isolation are also seen, generally attributed to the limited dispersal capacity of organisms. While this isolation effect is well established for oceanic islands, its applicability to continental island-like habitats is often weaker and more often disputed (e.g. Fahrig, 2013). This discrepancy may result from the greater permeability of the surrounding matrix, which facilitates rescue effects from the regional species pool via dispersal processes (Bender & Fahrig, 2005; Ricketts, 2001). Moreover, because isolation is often negatively correlated with the total amount of habitat in the landscape, the observed pattern may reflect a total-patch-area effect ('Habitat Amount') rather than isolation itself (Fahrig, 2003, 2013). As shown below, our study system offers a particularly suitable opportunity to explore contrasting predictions from the Habitat Amount Hypothesis, island biogeography and metacommunity theory in a tropical continental setting.

Island Biogeography Theory (IBT) provides a general framework for explaining species diversity patterns based primarily on the effects of area on extinction rates and of isolation on colonisation rates (MacArthur & Wilson, 1967). According to its predictions, colonisation rates decline with increasing isolation, while extinction rates rise as the habitat area decreases. Theoretically, these dynamics jointly regulate population sizes, determining equilibrium species richness through a balance of colonisation and extinction over time. Moreover, IBT also acknowledges that area can influence colonisation through the target effect, and that isolation can affect extinction via the rescue effect (MacArthur & Wilson, 1969).

Island biogeography has contributed to the development of new disciplines in spatial ecology (e.g. landscape ecology, macroecology and metacommunity ecology; see Presley & Willig, 2022). Despite its unquestionable success as a general ecological model and its significant influence on metacommunity and landscape ecology since its publication approximately 60 years ago (see Warren et al., 2015), IBT has also been widely criticised. One reason is that it does not consider habitat diversity and how this may modify how species are packed into a given area (Connor & McCoy, 1979). In addition, because it does not explicitly consider the effects of biotic interactions and the differences between species in relation to habitat choice and dispersive potential, IBT is taken as a purely stochastic theory, and forms a basis for other neutral theories (e.g. Hubbell, 2001). The assumption of 'functional equivalence between species' minimises the effects of biotic components (e.g. facilitation and competition) and environmental heterogeneity in the IBT and Neutral theory (see Hubbell, 2001) in favour of spatial processes controlling organism dispersion and support capacity in islands (MacArthur & Wilson, 1969).

Alternative hypotheses based on niche theory (Hutchinson, 1957) suggest that larger areas hold more species due to the indirect effect of area on habitat heterogeneity (Connor & McCoy, 1979; Fahrig, 2003, 2013; Hortal et al., 2009). Integrated frameworks that combine IBT and niche theory have recently begun to incorporate the role of environmental heterogeneity and biotic interactions (Allouche et al., 2012; Hortal et al., 2009; Kadmon & Allouche, 2007). While area, isolation and habitat heterogeneity are likely to jointly shape local community diversity, these studies revealed that the effect of environmental heterogeneity on species richness may be unimodal rather than a simple positive effect as previously thought (Allouche et al., 2012). This integrated approach further posits that average population abundance decreases—and thus stochastic extinction increases—as heterogeneity exceeds a threshold, because the effective habitat available for individual species declines, intensifying competition (Allouche et al., 2012; Kadmon & Allouche, 2007).

Modern metacommunity theory provides additional perspectives that emphasise different mechanisms—patch dynamics, mass effects, species sorting and neutral dynamics—to explain regional patterns of diversity and their effects on local diversity (Leibold et al., 2004). These models form a logical basis for linking processes across spatial scales within metacommunities, defined as 'a set of local communities linked by the dispersal of multiple potentially interacting species' (Leibold et al., 2004).

Natural continental island-like ecosystems provide valuable opportunities to test IBT and neutral predictions as stochastic models against niche-based expectations that incorporate environmental heterogeneity and biotic interactions. Within the tropics, savannas cover more land surface than any other biome and include some

of the most productive and diverse systems on Earth. In South America, for example, the extensive Brazilian Cerrado is recognised as a global biodiversity hotspot (Mittermeier et al., 2005), harbouring at least 12,103 seed plant species (BFG, 2015) and a wide variety of habitats. In the Cerrado, the ecological tension between grass-dominated habitats and areas locally dominated by trees depends on environmental features (Ribeiro & Walter, 2008). These tensions are only loosely controlled by climate, with local factors such as fire, flooding, nutrients and herbivory playing stronger roles. These generate remarkable habitat heterogeneity in some savanna regions, including island-like formations (Ratter et al., 2003).

An intriguing case of such island-matrix savanna formations occurs within seasonal floodplains in the Cerrado, known as *campos de murundus* (literally 'fields of earth mounds'; Figure 1 and Figure S1). These continental island habitats are dominated by trees and shrubs, and are formed through the combined action of multiple termite species that construct nests that are remodelled by abiotic processes, such as weathering, erosion and flooding, within a matrix of grasses and sedges (Furley, 1986; Marimon et al., 2015; Mathews, 1977; Oliveira-Filho, 1992a, 1992b; Ponce & Cunha, 1993). These three taxonomic groups—woody plants, herbaceous plants and termites—differ markedly in terms of their ecological traits relevant to biogeographical processes across spatial scales. Trees are long-lived and vary in dispersal limitations (e.g. autochoric, anemochoric and zoochoric), making them more sensitive to area and habitat heterogeneity than to isolation, as predicted by the IBT. Herbaceous plants, which typically produce abundant propagules dispersed by wind and water, may respond more strongly to microhabitat heterogeneity due to low dispersal limitations, aligning more closely with niche-based expectations. Termites, such as colonial social insects, may depend on specific nesting conditions and exhibit colony-driven spatial patterns, suggesting that local competition avoidance while new nests are established may outweigh simple area or isolation effects.

FIGURE 1 *Campo de murundus* (earth-mound field) sampled at the Araguaia State Park (ASP), Mato Grosso, Brazil. Each *murundu* island typically contains one or more termite nests located at its central, elevated portion. The surrounding flat area covered by grasses and herbs becomes seasonally flooded during the rainy period. Photograph: B. H. Marimon-Junior. The matrix is dominated by natural grasses.

Murundus islands arise from the initial establishment of termite colonies followed by multiple biotic and abiotic processes operating across scales, where some termite species act as ecosystem engineers, facilitating the colonisation of Cerrado plant species that are intolerant to water stress (Mathews, 1977). Consequently, gradients of island area, isolation and habitat heterogeneity shape the *murundus* landscape (Figure 1). The total habitat amount at the landscape scale also depends on interactions among biotic facilitation (through nest building), nest destruction by mammals and slow-changing abiotic factors. The *campos de murundus* occurs where the water table reaches the surface during the wet season (November–April), with *murundus* acting as islands that shelter termite nests and Cerrado species mostly intolerant to flooding (Marimon et al., 2015; Oliveira-Filho, 1992a, 1992b). Their distribution tends to be regular (Figures S1 and S2), a pattern indicative of competition avoidance among termite colonies (Mathews, 1977). Seasonal flood dynamics that isolate habitats during the rainy season and reconnect them during the dry season impose a pronounced seasonal rhythm on the ecosystem, which is consistent with the concept of hyperseasonal savanna (Batalha et al., 2005; Sarmiento, 1984). These dynamic savannas restrict both organisms who are intolerant of water-saturated soils and those unable to store water during extremely dry periods (Oliveira-Filho, 1992a, 1992b). The flooding period imposes constraints on survivors of termite species, which can become locally extinct if the nest did not grow sufficiently to escape the water level, which is climatically controlled.

Multiple abiotic and biotic processes contribute to the formation of *murundus* fields, and their relative importance varies according to topography and landscape water stress (Furley, 1986; Marimon et al., 2015; Mathews, 1977; Oliveira-Filho, 1992a; Ponce & Cunha, 1993; Silva et al., 2010). In flat, seasonally flooded areas, biotic factors initiate *murundus* formation through termite colonisation during the dry season (Marimon et al., 2015; Mathews, 1977; Oliveira-Filho, 1992a). Termite species richness changes with *murundus* maturation as environmental conditions evolve with mound growth (see Davies et al., 2016). This activity facilitates colonisation by many woody and herbaceous species otherwise susceptible to flooding, underscoring the importance of these indirect termite–plant interactions in shaping these systems (Marimon et al., 2012, 2015; Mathews, 1977; Oliveira-Filho, 1992a, 1992b).

The effect of *murundus* area on tree species richness has been documented in seasonally flooded savannas in Central Brazil (Oliveira-Filho, 1992a, 1992b) and Africa (Davies et al., 2016). However, two key components of island habitats—environmental diversity and isolation—were not explicitly considered in these studies. As multiple abiotic and biotic factors interact during *murundus* development (Mathews, 1977; Oliveira-Filho, 1992a; Ponce & Cunha, 1993), it is crucial to evaluate how dispersal mechanisms and physical features (e.g. habitat amount, island size, volume and height) interact with their key biological agents—termites and plants.

Most studies on species–area relationships have focused on patterns arising from colonisation and the development of quasi-independent biotas on oceanic islands or isolated continental fragments (e.g. lakes, ponds, mountaintops and reservoir islands).

Here, we examine three taxonomic groups—trees, herbaceous plants and termites—because of their ecological relevance in *murundus* fields and their contrasting biological traits, which make them, especially suitable for assessing the roles of area, isolation and habitat heterogeneity. These groups were also selected because their populations and communities are structured at spatial scales that match the extent of our study landscape, allowing them to respond detectably to the predictors evaluated, unlike highly mobile organisms, such as mammals whose dynamics operate at broader spatial scales. Trees and herbaceous plants are sessile primary producers whose establishment and persistence depend on local environmental conditions, total habitat amount and spatial constraints on seed recruitment. Importantly, our landscape encompasses all the sampled habitat patches, enabling rigorous tests of Habitat Amount Hypotheses. In contrast, termites are recognised ecosystem engineers that construct nests and shape *murundus* formation in synergy with abiotic and biological processes (e.g. mammalian predation on termites). Their colony-based lifestyle makes them particularly relevant for understanding how biotic and abiotic interactions influence community assembly. For termites, the amount of habitat may be partially related to patch size but may be more strongly related to local nest characteristics. Given these functional differences, we expect the processes emphasised by IBT, metacommunity theory and the Habitat Amount Hypothesis to influence each group differently. These mechanisms are not mutually exclusive and may act jointly to shape species richness patterns.

Our a priori hypotheses for the inference of the importance of each theory are as follows. First, tree species are influenced positively by area because small islands suffer stochastic extinction more often (1), because larger targets increase the chance of seed arrival and recruitment, and sampling effects (the larger the area, the greater the sample size). Habitat heterogeneity has a secondary effect mediated by area, reflecting *species-sorting* mechanisms related to niche theory under competition for limited resources. Second, herbaceous species, which produce numerous wind-dispersed propagules and occupy diverse microhabitats, respond positively to *murundus* area rather than isolation (2), consistent with mass effects where seed input from larger or more productive islands and the regional landscape enhances local diversity, Third, termite assemblages, which are composed of sessile, colony-forming social insects with limited dispersal, primarily reflect spatial dynamics and competitive avoidance rather than *murundus* area or isolation, and are driven instead by local habitat availability (3). The number of nests is expected to determine termite richness, whereas *murundus* height may influence population persistence, as lower mounds are more prone to flood-driven extinction. Finally (4), we expect *murundu* landscapes to produce emergent metacommunity patterns, with vegetation (trees and herbs) depending more on the total habitat amount, whereas termites depend more on local conditions and the *murundus* distribution pattern in the landscape. These distinct mechanisms, if confirmed by our theory-based analytical approach of observations across the *murundus* landscape, would illuminate the processes governing species diversity and coexistence in hyperseasonal savannas, as well as clarifying the relative effects of the Habitat Amount Hypothesis, landscape structure, fragmentation and metacommunity drivers for each of these distinctive organism groups.

2 | MATERIALS AND METHODS

2.1 | Study area

We conducted this study in the Araguaia State Park (ASP), in north-eastern Mato Grosso state, central Brazil, between 11°43′ S, 50°43′ W and 12°38′ S, 50°49′ W (Figure 2). The ASP covers approximately 223,000 ha and forms part of the largest continuous wetland in Brazil, which spans approximately 90,000 km^2 (Martini, 2006). Over 80% of the ASP consists of *murundu* fields; however, it also contains other savanna and forest formations (Marimon et al., 2008, 2015; Marimon & Lima, 2001). The regional climate is classified as a savanna subtype (Köppen's Aw), characterised by a rainy summer (November–April) and a dry winter (May–October). The mean annual precipitation is approximately 1600 mm, and the mean temperature is approximately 25°C (Marimon & Lima, 2001). Further details of the study area are provided by Marimon et al. (2008, 2012, 2015). Permissions to access the research area and conduct the research at ASP (PEA), as well as to use the PEA administrative headquarters for accommodation and research support, were granted by the Mato Grosso State Secretariat for the Environment (SEMA).

2.2 | Experimental design and biotic groups sampling

We established 11 discontinuous 100 × 100 m plots (1 ha each; total area of 110,000 m^2), within which we sampled and mapped 373 *murundus*. The number of *murundus* per hectare plot ranged from 15 to 51. Within each *murundu*, we recorded and identified all the plants (trees, shrubs, sub-shrubs, palms, lianas and herbs), excluding grasses (Poaceae) and sedges (Cyperaceae) (Marimon et al., 2012, 2015). Comprehensive lists of plant species, as well as details of the botanical collection and identification procedures, are available in Marimon et al. (2012, 2015).

Termites were sampled from each *murundu* as follows: nests—from each nest, we collected at least five fragments from three different positions and heights, transferred them to white sorting trays and collected all the termites present for 10 min; soil—four soil samples were taken, and the termites were collected via the same procedure. All termite collections were preserved in 70% ethanol in labelled vials and transported to the Termite Laboratory of the University of Brasília (Federal District, Brazil) for identification.

The plants were classified into two groups: (i) trees, shrubs, palms and lianas with diameter measured at 30 cm from the ground ($D_{30\,cm}$) ≥3 cm (hereafter 'trees'); and (ii) sub-shrubs and herbs with $D_{30\,cm}$

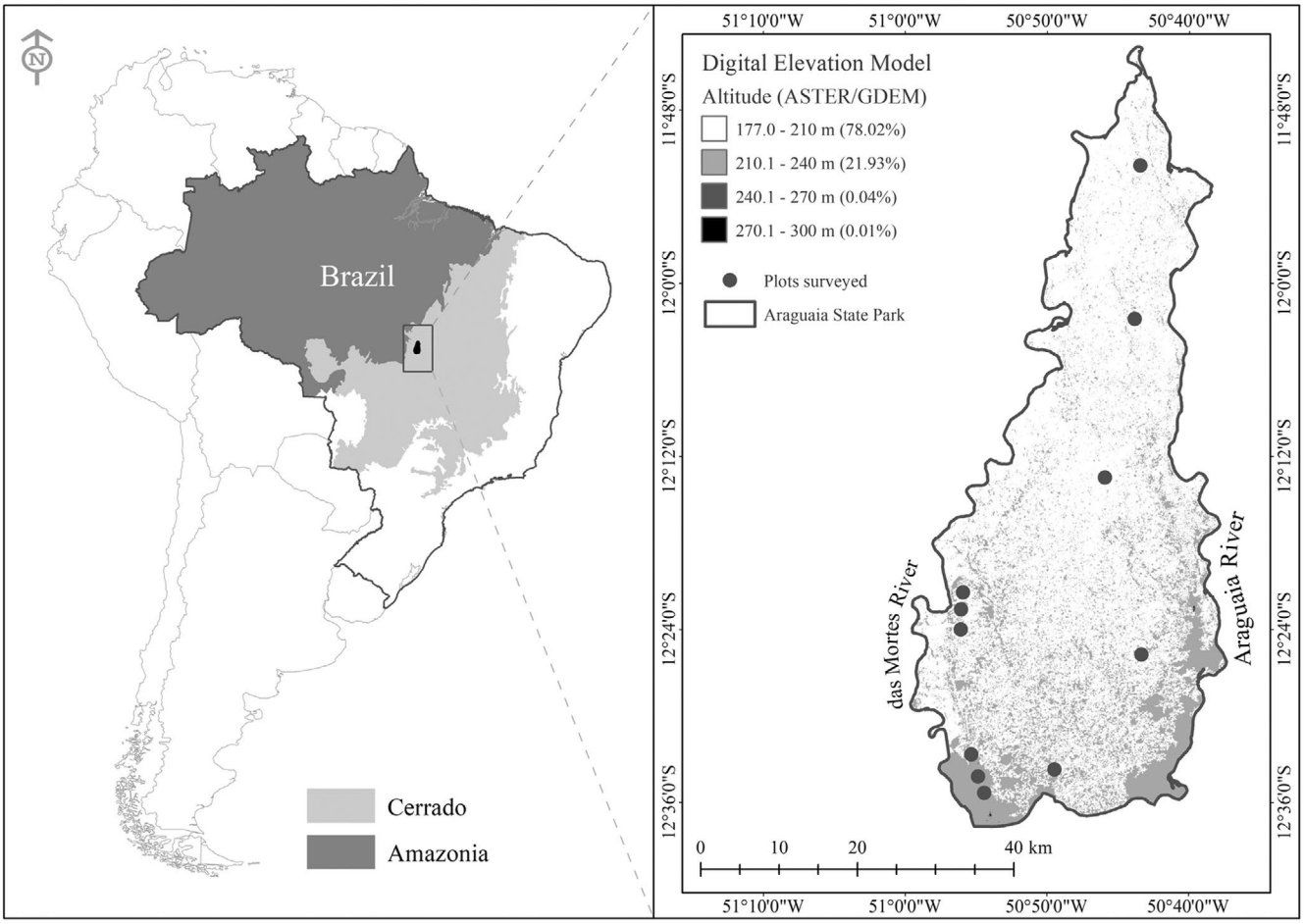

FIGURE 2 Eleven 1-ha plots of *campo de murundus* (earth-mound fields) sampled in Araguaia State Park (ASP), Mato Grosso, Brazil, showing their locations relative to the Cerrado and Amazonia biomes. The das Mortes River (west) and Araguaia River (east) delimit the ASP. The digital elevation model (ASTER/GDEM; spatial resolution 30 m) illustrates four elevation classes above sea level and their respective susceptibilities (%) to seasonal flooding.

<3 cm (hereafter 'herbs'). We then constructed five data matrices: (i) trees, (ii) herbs, (iii) termites, (iv) spatial coordinates (*x* and *y*) of each *murundu* and (v) environmental predictors. The tree and termite matrices contained species abundance data, whereas the herb matrix contained presence–absence data. From these three biotic matrices, we calculated the estimated species richness and distribution across all 373 *murundus* samples.

As predictors of variation in species richness, we used (i) *murundus* area, (ii) isolation among *murundus* and (iii) environmental heterogeneity. The *murundu* area (m^2) was estimated by modelling each mound as a semi-ellipse, following the equation proposed by Oliveira-Filho (1992a). Isolation was quantified as the distance from the centre of each *murundu* to its nearest neighbour and to the largest nearby *murundu*. We measured the height of each *murundu* (at its centre) relative to the adjacent grass-dominated flatland and used this height, together with mound volume (m^3), as a measure of habitat heterogeneity for trees and herbs. For termites, habitat heterogeneity was estimated from the number of nests on each *murundu* combined with its height, as both factors influence species settlement (Mathews, 1977; see below).

2.3 | Data analysis

All the statistical analyses were performed in R, version 4.5.0 (R Core Team, 2025). Our primary objective was to model the species richness of three taxonomic groups (trees, herbs and termites) as a function of local environmental predictors (e.g. *murundu* area and habitat heterogeneity) and spatial configuration, represented by spatial filters derived from *murundus* centroid coordinates. At the landscape scale, we tested the Habitat Amount Hypothesis by examining the effects of the total *murundus* area, the number of *murundus* (used as a *proxy* for metacommunity size), and the mean inter-*murundu* distance within plots on the total abundance and observed species richness summed at the plot level for each taxonomic group.

2.3.1 | Habitat heterogeneity and availability

To evaluate habitat heterogeneity, we used the median distance to the centroid obtained from a multivariate homogeneity of group dispersion analysis (PERMDISP; Anderson et al., 2006), which was

applied in two distinct ways to reflect biological differences between plants and termites. For plants (herbs and trees), habitat heterogeneity was estimated via the *murundu* island volume (m^3) and height (m) relative to the surrounding grassland matrix up to the top of the *murundu*—excluding the termite nest itself. For termites, it was based on the number of termite nests per *murundu* island and the *murundu* height (m). We used Euclidean distances among standardised variables for all pairs of *murundus* within the 11 sampled 1-ha plots. Additionally, we compared the environmental heterogeneity among the plots via Permutational Multivariate Analysis of Variance (PERMANOVA) with the adonis function (Anderson, 2001) and performed PERMDISP with the betadisper function from the vegan package (Oksanen et al., 2018), employing 9999 unrestricted Monte Carlo permutations. Habitat heterogeneity and availability for plants (hereafter, heter.veg) and termites (hereafter, heter.termites) were represented by the distance to centroid values obtained for each of the 11 1-ha plots. Statistics summarising the distribution of the observed values for the original predictors (e.g. area, distance, volume and height), as well as for the derived measures of habitat heterogeneity and availability, were calculated and plotted via the 'ggpairs' function from the 'GGally' package (Schloerke et al., 2025), to examine their correlations.

2.3.2 | Diversity estimates

We plotted interpolation and extrapolation curves based on the Hill series (order $q=0$), with no weighting for species abundance. We focused on species richness estimates because they are directly related to the IBT and Habitat Amount Hypothesis, although we acknowledge that higher-order diversity measures (Shannon and Simpson effective diversity) can provide additional insights and are less affected by incomplete sampling coverage (Chao et al., 2014). Nevertheless, we restricted our analyses to species richness to ensure interpretability within the framework of these classic theories and for brevity. We also used sample coverage to assess differences in sampling completeness among the studied communities (Chao et al., 2014; Chao & Jost, 2012; Colwell et al., 2012). Asymptotic Chao species richness estimates were used as the main response variable for each taxonomic group, since observed species richness is often underestimated (Chao et al., 2014; Chao & Jost, 2012; Colwell et al., 2012). Rarefaction and extrapolation curves, asymptotic species richness estimates and sampling coverage calculations were implemented via functions from the 'iNEXT' package (Hsieh et al., 2018).

2.3.3 | Generalised linear mixed models

We evaluated the effects of area, distance to the nearest large neighbour and environmental heterogeneity on *murundus* species richness for the three biotic groups using generalised linear mixed models (GLMMs) with a negative binomial distribution, which is appropriate for over-dispersed ecological count data, implemented with the glmer.nb() function from the 'lme4' package (Bates et al., 2015). The 11 *murundus* fields were included as random effects. We $\log_{10}$-transformed area and distance metrics to minimise potential biases arising from differences in measurement scales among predictors and centred all fixed predictors to control for multicollinearity. However, diagnostic tests of model assumptions conducted with the performance package (Lüdecke et al., 2021) revealed significant residual spatial autocorrelation ($p=0.001$), poor posterior predictive checks (PPCs) and evidence of mis-specified dispersion and zero inflation across the taxonomic groups (see the Bayesian Regression Model Checking section in the Supporting Information). We therefore used nested Moran's Eigenvector Maps (MEMs) to account for residual spatial autocorrelation and to capture the spatial structure of *murundus* distributions across the landscape in relation to species richness (detailed below).

2.3.4 | Spatial structure modelling: Nested Moran's Eigenvector Maps

To account for spatial autocorrelation across multiple spatial scales, we employed MEMs. Given that our sampling design was hierarchical, with *murundus* nested within 11 1-ha plots, we generated MEMs that respected this nested structure. First, we calculated a matrix of Euclidean distances from the spatial coordinates of each *murundu*. Next, we defined a connectivity matrix by truncating the distance matrix at a threshold corresponding to the minimum distance required to ensure that all *murundus* remained connected within a single spatial network. This threshold was determined via the 'dbmem' function from the 'adespatial' package (Dray et al., 2023). The principal coordinates of this truncated distance matrix were then computed, producing a complete set of MEM variables that capture orthogonal spatial patterns ranging from broad-scale gradients to fine-scale spatial patches (Dray et al., 2006).

2.3.5 | MEM selection and model simplification

After computing the MEMs, we employed a two-step selection procedure to identify the most relevant subset of MEMs for inclusion in the final models, thereby avoiding overfitting. First, the residuals from the baseline negative binomial GLMM—fitted with the key environmental predictors (log(Area), log(Dist), Heter.veg, log(Dist_Big)) as fixed effects and Plots as a random intercept term to account for the nested sampling design—were used for initial MEM selection. Second, we applied a forward selection procedure implemented in the forward.sel function of the 'adespatial' package via a double–stopping criterion (Bauman, Drouet, et al., 2018; Bauman, Fortin, et al., 2018; Blanchet et al., 2008). This step sequentially retained only the significant spatial eigenvectors, optimising the computationally intensive selection process while preventing overfitting and maintaining statistical power to detect the environmental

contribution to the variation in species richness. Further details are provided in the documentation of mem.select within the 'adespatial' package and in the cited references.

This procedure iteratively incorporated MEMs into the baseline model, retaining only those that significantly accounted for the residual spatial structure while most accurately capturing the spatial patterns of species richness (Bauman, Fortin, et al., 2018). Following this pre-selection step, we undertook a model simplification process using the dredge function from the 'MuMIn' package (Bartoń, 2018). This all-subset model selection was applied to a global model containing pre-selected MEMs and the fixed environmental predictors. The environmental predictors were specified as fixed terms to be retained in all the candidate models, thereby ensuring that the selection process focused solely on optimising the set of spatial predictors. The best-fitting model was identified as the one with the lowest Akaike Information Criterion corrected for small sample sizes (AICc) (Akaike, 1974; Burnham & Anderson, 2002; Diniz-Filho et al., 2008). The explanatory power of our GLMMs was assessed via both marginal and conditional coefficients of determination (R^2_m and R^2_c, respectively; Nakagawa & Schielzeth, 2013). The R^2_m represents the variance explained solely by the fixed effects (i.e. the environmental and spatial predictors), whereas the R^2_c represents the variance explained by both the fixed and random effects combined (i.e. the variation among plots; Nakagawa & Schielzeth, 2013). A large difference between R^2_c and R^2_m indicates that a substantial portion of the variation in species richness is attributable to baseline differences among the *murundus* fields (plots), highlighting the importance of accounting for this hierarchical structure. The R^2_m, in turn, quantifies the explanatory power and generality of the ecological predictors after controlling for this inter-plot variability. We calculated the R^2 values for random and fixed effects via the 'MuMIn' package (Bartoń, 2018).

Despite better control over residual spatial autocorrelation ($p = 0.002$), variance homogeneity, residual normality and random effects, diagnostic checks of the models, including both environmental and spatial predictors remained problematic. These issues included residual autocorrelation, poor fit in PPCs, mis-specified dispersion and zero inflation, as well as convergence failures.

2.3.6 | Bayesian generalised linear mixed-effects models

For the final analysis and parameter estimation, we re-implemented the best-fitting GLMMs within a Bayesian framework via the 'brms' package (Bürkner, 2017, 2018, 2021), which provides an interface to the probabilistic programming language Stan (Stan Development Team, 2023). This approach offers several advantages, including robust accommodation of complex model structures and intuitive quantification of uncertainty through posterior distributions. Although traditional hypothesis testing remains valuable in controlled experiments with few parameters, there is some concern about the frequentist use of probability tests and increasing recommendations for Bayesian inference (e.g. Bürkner, 2021). In addition, the complexity of our system has proven challenging to capture via frequentist approaches, such as '*lmer*', '*gamm*' and '*glmmTMB*' (Brooks et al., 2017; McGillycuddy et al., 2025). The use of 'BRMs' provided greater flexibility in specifying mixture distributions to address zero inflation (present in herbs and termites), while enabling the estimation of effect sizes and their precision without convergence issues. To accommodate group-specific characteristics, we employed a negative binomial distribution for estimated tree species richness (Richness ~ negbinomial), whereas herbs and termites were modelled using a hurdle negative binomial distribution (Richness ~ hurdle_negbinomial). Hurdle negative binomial gives the probability of each individual *murundu* island having absence (zero) or presence of species (hu), while the negative binomial models the expected number of species among *murundus* with presence of species only, which was adjusted for heterogeneity variance among small islands (via shape term). The BRM models were well supported by gam models fitted with 'mgcv' package with random effects with the same error distribution. BRM model assumptions were checked using appropriate Bayesian statistics and graphics from the 'brms' and 'bayesplot' packages and described in the Supporting Information (Tables S2–S4; Figures S7–S12).

2.3.7 | Landscapes-metacommunity drivers of α-diversity

The spatial patterns in hyperseasonal island-habitat landscapes are derived from biological processes that emerge from interactive engineering among termites, vegetation, mammals and physical factors during the successional development of *murundus* fields. It is expected that this pattern did not arise at random but conforms to regularity in the spatial distribution of *murundu* islands, as suggested by previous evidence (e.g. Marimon et al., 2015; Mathews, 1977) and by observations in the field and from satellite images (see the Supporting Information). We visually inspect this pattern via the classical Ripley's *K* statistic (Ripley, 1977) and test the hypothesis of complete spatial randomness (CSR) in island point patterns formally via a modification of the original Ripley's *K*, the maximum absolute deviation (MAD), and derivations proposed to improve this seminal work (Cressie, 1991; Diggle, 1986; Loosmore & Ford, 2006). These authors and recent studies claim that MAD may be conservative if it is to be estimated from observed data with the original formulation of Ripley's *K* (Brunsdon & Comber, 2019; see Baddeley et al., 2015). Accordingly, we take the set of spatial coordinates of all individual islands within each *murundu* landscape (11 1-ha plots) and apply the Diggle–Cressie–Loosmore–Ford (DCLF) test of CSR, with the linear statistic for *dclf.test* function of the 'spatstat' package to identify directional trends towards the hypothesis of regularity (setting alternative = 'less'; Baddeley et al., 2015). The linear function formula is defined as follow:

$$L(r) = \sqrt{\frac{K(r)}{\pi}}, \quad (1)$$

where $K(r)$ is Ripley's K at a circle of radius r (Besag, 1977; Brunsdon & Comber, 2019).

The MAD and DCLF tests of CSR with *Lest* statistics yield similar results, and only the latter is used to represent a landscape structure variable of spatial regularity at the plot scale (Figure S3; Table S1).

We calculated the habitat amount as the sum of all *murundu* island areas at the plot scale. For landscape structure, we calculated the average *murundu* area, average distance among all islands, average distance among large islands and proximity index (island area/average island distance within plots). Habitat fragmentation was defined by the number of islands and island density within the plots. Finally, we inserted metacommunity scale parameters (total abundance, beta diversity and gamma diversity) as predictor links for Bayesian Structural Equation Models (BSEMs).

The rationale for including emerging patterns in landscape–metacommunity theory emphasises the interaction of multiple-scale processes that may influence local diversity (α-diversity). In neutral metacommunity dynamics, the fundamental biodiversity parameter (θ) depends on the total abundance of species in the metacommunity (J) and the speciation rate (ν) (Hubbell, 2001). The parameter J is estimated directly from the sum of the island abundances of all species on each *murundu* island as follows:

$$J_i = \sum_{i=1}^{S} n_i, I, \tag{2}$$

where n_i, I is the abundance of species i in the local I, and S is the number of species in the local I.

Analogously, the size of a metacommunity (J_m) is as follows:

$$J_m = \sum_{I=1}^{L} J_I, \tag{3}$$

where L is the number of sites.

In a neutral model, the expected α-diversity is a function of θ and J:

$$E[S] = \theta \sum_{k=1}^{J} \frac{1}{\theta + k - 1}, \tag{4}$$

where $\theta = 2J_m\nu/(1-\nu)$ (Hubbell, 2001).

An increase in J and θ increases the chance of higher α-diversity. Given that we do not have an effective measure of the speciation rate for any taxon to accurately estimate θ, we used the parameter J log-transformed (*logJ*) and plot scale Chao species richness estimates (as a proxy for γ-diversity) to infer metacommunity fundamental biodiversity effects on local diversity patterns.

We defined α-diversity as the local Chao species richness estimated ($S_{[Chao]}$) at the island scale and then averaged it within plots. The effect of γ-diversity on α-diversity is somehow dependent on the magnitude of environmental control on β-diversity, owing to turnover if there are positive niche effects on the spatial distribution of species, consequently increasing γ-diversity, or to nestedness if the effect of area solely relates to the sampling effect or target effect with smaller islands as subsets of the diversity of the largest islands. Beta diversity was calculated via the multiplicative formulation of Whittaker (1960):

$$\beta = \frac{\gamma}{\tilde{\alpha}}, , \tag{5}$$

For these aggregated data at 11 1-ha plots, we fit the BSEMs with Gaussian distributions and linked logarithms to assess the individual, direct and indirect effects of the models on alpha diversity: (1) habitat amount, (2) landscape structure, (3) fragmentation and (4) metacommunity (scaled gamma diversity, beta diversity and the logJ parameter). The indirect effects of habitat amount, landscape structure and habitat fragmentation on metacommunity parameters were tested for Models 1–3. For Model 4, only metacommunity parameters were considered, and indirect effects of *logJ* on γ-diversity and γ-diversity on β-diversity were also considered.

3 | RESULTS

3.1 | Physical properties of the *murundus* fields

We encountered a total of 373 *murundus* in the 11 1-ha plots, with individual areas varying from 0.12 to 121.6 m^2, and total plot-level *murundu* area ranging from 811 to 1432 m^2 (Figure S2). The nearest-neighbour distances ranged from 3.9 to 36 m among all *murundus* and from 4.6 to 36 m among the large *murundus*. The spatial distribution of *murundus* was clearly non-random within most plots (Table S1), with the observed values of Ripley's K-function consistently smaller than those expected under the CRS distribution (Figure S3).

We detected active termite nests in 99.6% of the *murundus*, but the number of nests varied greatly (0–13/*murundu*), and this number was weakly correlated with the *murundu* area (Figure S4), which we used as an independent predictor of habitat heterogeneity/availability for termites. The correlations between the predictors and island area were generally moderate to low (rho ≤ 0.60), except for the strong, non-linear positive associations between the *murundu* area, volume and height (rho = 0.68–0.94; Figure S4), resulting in increasing environmental heterogeneity as *murundus* became larger when the plant-related variables were considered (rho = 0.71). The environmental heterogeneity varied widely among *murundus* of different sizes (Figure S4). Most *murundus* were small (ca. 2.5 m^2), had intermediate nearest-neighbour distances (ca. 13 m), contained a single termite nest, had moderate height (0.9 m) and exhibited low habitat heterogeneity (Euclidean distance to the Betadisper centroid, ca. 1.1 to 12.1, for termites and vegetation, respectively). In addition, environmental heterogeneity differed significantly among plots and in terms of dispersion to the centroid for vegetation (adonis $R = 0.180$, $F_{(10, 362)} = 7.959$, $p = 0.001$; betadisper $F_{(10, 362)} = 2.261$, $p = 0.014$, respectively) and for termites (adonis $R = 0.355$, $F_{(10, 362)} = 19.971$, $p = 0.001$; betadisper $F_{(10, 362)} = 9.970$, $p < 0.001$, respectively; Figure S5A,B).

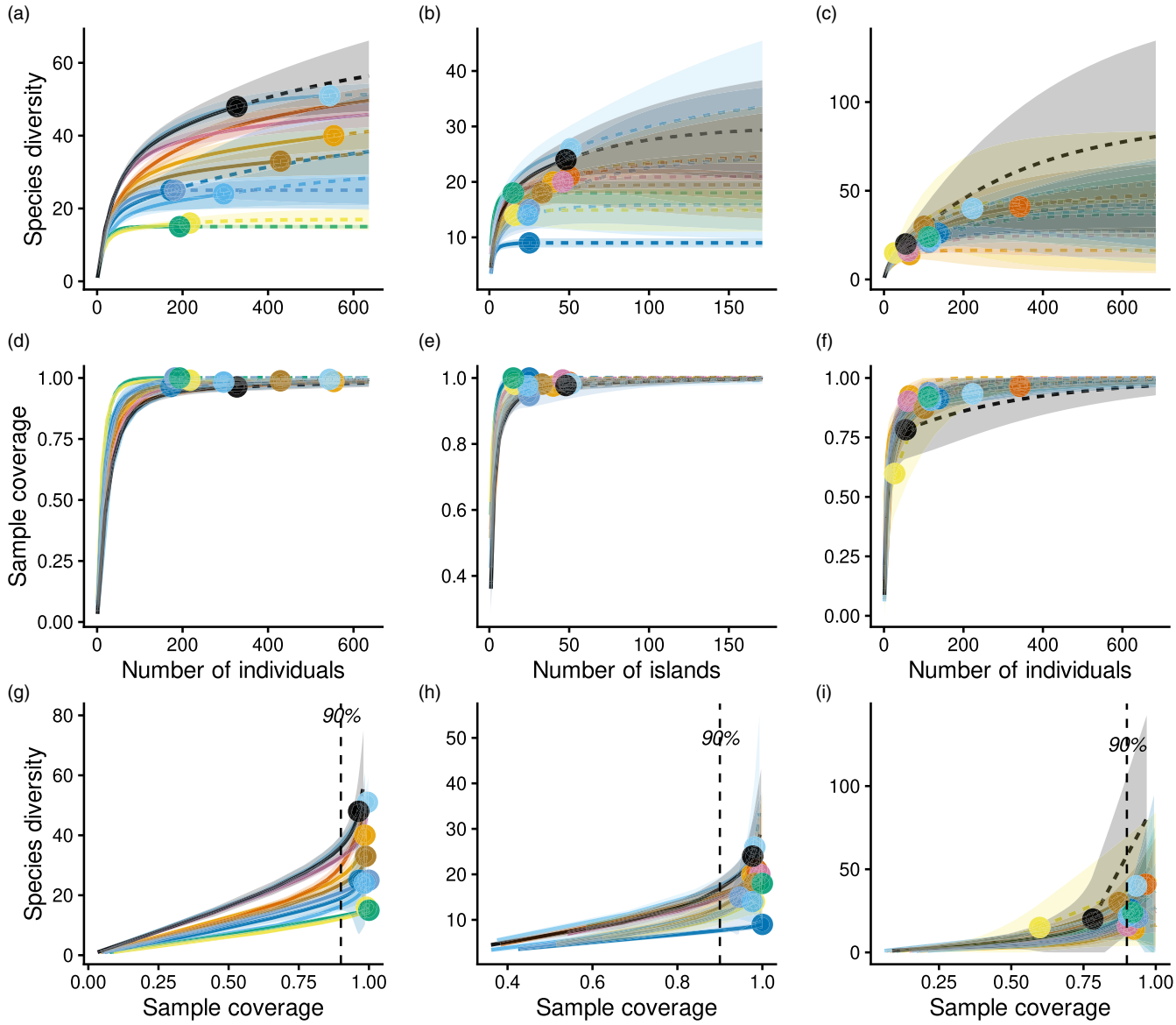

FIGURE 3 Species diversity analyses across 11 1-ha plots of *murundu* fields sampled in Araguaia State Park, Mato Grosso, Brazil, showing individual-based rarefaction and extrapolation curves for order $q = 0$ (a–c), sample-coverage curves as a function of the number of individuals sampled (d–f), and species diversity plotted against sample coverage (g–i) for trees (a, d, g), herbs (b, e, h) and termites (c, f, i). Each colour denotes one 1-ha plot.

3.2 | Metacommunity patterns

In total, we sampled 250 species distributed among trees (98 species), herbs (80) and termites (72). Total species richness varied from one to 21 per individual *murundu*, and from 17 to 56 across the 11 1-ha plots (Figure 3a; Table 1). At the individual *murundus* level, tree species richness ranged from zero to 18, herb richness ranged from nine to 51, and termite richness ranged from zero to 13 species (Figure 3a–c; Table 1). Trees were recorded in 99% of all *murundus*, herbs in 96% and termites in 86%. Regarding sampling effort, both trees and herbs presented high sample completeness across all *murundus* fields, with coverage values ranging from 95.9% to 98.9% for trees and from 94.6% to 100% for herbs (Table 1). In contrast, termite sampling coverage was more heterogeneous among plots, ranging from 59.8% to 96.5%, reflecting greater uncertainty in richness estimates for *campo de murundus* CM2, CM6 and CM9 (Table 1; Figure 3). For all the taxonomic groups, the shape of the density distribution followed a known left-skewed pattern of abundance and species counts, whereas the magnitude of the rare species concentration varied among them (Figure S6).

3.3 | Drivers of local species richness

3.3.1 | Trees

At the local community scale, the set of predictors tested (area, isolation and environmental heterogeneity), along with

Plots	Trees			Herbs		Termites		
	Cov	Ric	Abu	Cov	Ric	Cov	Ric	Abu
CM1	98.2	43	554	97.5	20	92.5	14	65
CM2	98.6	28	217	97.9	14	59.8	15	27
CM3	97.7	17	173	100.0	9	91.3	26	137
CM4	98.6	40	661	98.7	21	96.5	41	342
CM5	98.9	45	661	99.4	20	90.3	16	61
CM6	98.6	41	429	98.0	18	87.2	30	101
CM7	96.7	24	182	94.6	15	93.9	21	113
CM8	97.2	56	544	98.2	26	93.3	40	223
CM9	96.6	44	327	97.7	24	78.2	20	55
CM10	98.7	34	296	97.6	14	90.6	22	117
CM11	95.9	22	193	100.0	18	92.0	24	112
Plots range	0.2–1.0	1–21	1–63	0.1–0.8	0–18	0.2–1.0	0–13	0–21

Abbreviations: Abu, abundance; Cov, sample coverage (%); Ric, observed richness.

TABLE 1 Sample coverage (%), species richness and abundance of trees, herbs and termites in 11 1-ha plots of *campo de murundus* (CM) sampled in Araguaia State Park, Mato Grosso, Brazil.

TABLE 2 Results from Bayesian generalised mixed-effects mixture models for estimated tree species richness via a hurdle negative binomial distribution.

Terms	Estimate	SE	L-CI	U-CI	Rhat	Bulk_ESS	Tail_ESS
Intercept	2.04	0.13	1.79	2.29	1.00	2261	3346
shape_Intercept	1.51	0.17	1.20	1.86	1.00	5339	5194
Area	**0.79**	**0.04**	**0.71**	**0.86**	**1.00**	**5304**	**5407**
Distance	−0.17	0.15	−0.47	0.13	1.00	5308	5476
Heterogeneity	−0.02	0.02	−0.06	0.03	1.00	5226	5053
MEM_PlotCM10_10	**0.43**	**0.12**	**0.20**	**0.66**	**1.00**	**4840**	**4896**
MEM_PlotCM6_19	**−0.29**	**0.09**	**−0.47**	**−0.13**	**1.00**	**4828**	**5024**
MEM_PlotCM4_20	**0.21**	**0.09**	**0.02**	**0.40**	**1.00**	**4841**	**4899**
MEM_PlotCM8_22	**0.23**	**0.09**	**0.06**	**0.40**	**1.00**	**5355**	**5105**
MEM_PlotCM4_33	**0.29**	**0.09**	**0.11**	**0.46**	**1.00**	**4926**	**5105**
MEM_PlotCM9_23	−0.16	0.09	−0.34	0.01	1.00	5135	4869
MEM_PlotCM4_25	**−0.19**	**0.09**	**−0.38**	**−0.01**	**1.00**	**5226**	**4966**
MEM_PlotCM4_30	**−0.20**	**0.09**	**−0.37**	**−0.02**	**1.00**	**4658**	**5138**
MEM_PlotCM4_39	−0.15	0.09	−0.32	0.03	1.00	4959	5148
MEM_PlotCM4_24	**−0.24**	**0.10**	**−0.45**	**−0.04**	**1.00**	**4970**	**4888**
MEM_PlotCM5_23	**0.22**	**0.08**	**0.06**	**0.37**	**1.00**	**4918**	**4574**
MEM_PlotCM4_43	−0.14	0.08	−0.29	0.02	1.00	4895	5324
MEM_PlotCM4_13	−0.15	0.09	−0.34	0.02	1.00	5072	5211
Shape heterogeneity	0.06	0.06	−0.06	0.17	1.00	5180	5208

Note: Significant terms, based on their 95% confidence intervals, are shown in bold.

Abbreviations: L-CI, lower 95% confidence interval; SE, standard error; U-CI, upper 95% confidence interval.

multi-scale MEMs nested within plots, explained 66% of the variation in estimated tree species richness ($R^2 = 0.657 \pm 0.028$; CI = 0.598–0.707). The primary driver of tree species richness was *murundu* island area (Table 2). Several intermediate- and fine-scale MEMs were associated with tree species richness, increasing model complexity as indicated by the high information criterion (LOOIC = 2253.6), but were necessary to account for residual spatial autocorrelation and satisfy normality assumptions. Isolation and environmental heterogeneity did not significantly explain tree species richness. The exclusion of area while retaining all other predictors drastically reduced the model's performance (ΔLOOIC = 298.7 ± 34.1). Overall, a 10% increase in the

TABLE 3 Results from Bayesian generalised mixed-effects mixture regression models (BRMs) for estimated herb species richness via a hurdle negative binomial distribution.

Terms	Estimate	SE	L-CI	U-CI	Rhat	Bulk_ESS	Tail_ESS
Intercept	2.32	0.18	1.96	2.69	1.00	1259	2213
shape_Intercept	0.82	0.19	0.45	1.19	1.00	3023	2911
hu_Intercept	−4.21	0.50	−5.34	−3.33	1.00	3195	3389
log_Area	**0.69**	**0.05**	**0.59**	**0.79**	**1.00**	**3366**	**3547**
log_Dist_Big	0.11	0.19	−0.28	0.49	1.00	3741	3492
log_Heter_veg_center	0.07	0.04	−0.02	0.16	1.00	2870	3350
MEM_PlotCM10_10	−0.09	0.14	−0.38	0.20	1.00	3613	3114
MEM_PlotCM6_19	−0.02	0.13	−0.29	0.23	1.00	3340	3334
MEM_PlotCM8_49	**0.20**	**0.08**	**0.05**	**0.37**	**1.00**	**3508**	**3463**
MEM_PlotCM8_11	**−0.24**	**0.08**	**−0.41**	**−0.07**	**1.00**	**3527**	**3475**
MEM_PlotCM3_18	−0.34	0.19	−0.72	0.02	1.00	3608	3586
MEM_PlotCM5_23	0.14	0.09	−0.05	0.32	1.00	3261	3336
MEM_PlotCM4_43	−0.15	0.10	−0.35	0.05	1.00	3435	3045
shape_log_Heter_veg_center	**0.26**	**0.10**	**0.04**	**0.45**	**1.00**	**2883**	**3427**
hu_log_Area	**−1.23**	**0.31**	**−1.87**	**−0.66**	**1.00**	**3266**	**3661**
hu_log_Dist_Big	0.17	0.75	−1.27	1.66	1.00	3595	3389
hu_log_Heter_veg_center	0.27	0.23	−0.14	0.74	1.00	3543	3598
hu_MEM_PlotCM3_18	0.01	0.77	−1.49	1.51	1.00	3676	3628
hu_MEM_PlotCM4_43	0.02	0.69	−1.35	1.33	1.00	3618	3388
hu_MEM_PlotCM6_8	−0.70	0.69	−2.03	0.70	1.00	3784	3678
hu_MEM_PlotCM8_11	−0.26	0.54	−1.35	0.81	1.00	3707	3369
hu_MEM_PlotCM8_21	−0.22	0.52	−1.22	0.84	1.00	3657	3197
hu_MEM_PlotCM8_49	−0.31	0.60	−1.47	0.85	1.00	3856	3699
hu_MEM_PlotCM9_4	−0.21	0.57	−1.30	0.94	1.00	3458	3496

Note: Credible terms based on their 95% confidence intervals are shown in bold.

Abbreviations: L-CI, lower 95% confidence interval; SE, standard error; U-CI, upper 95% confidence interval.

murundu area resulted in a 7.8% increase in tree species richness (95% CI: 7.0–8.6).

3.3.2 | Herbs

For herbs, the predictors (area, isolation and environmental heterogeneity), along with medium- to fine-scale MEMs nested within plots, explained 63% of the variation in estimated herb species richness ($R^2 = 0.628 \pm 0.037$; CI = 0.533–0.686; LOOIC = 2572.8 ± 48.1). The main driver of herb species richness was again the *murundu* island area (+0.69; CI = 0.59–0.79; Table 3). We found strong evidence that area was the main predictor of herb species richness, since the model run without area presented a substantially greater LOOIC (ΔLOOIC = 142.4 ± 24.8). An increase of 10% in the *murundu* area resulted in a 7% increase (95% CI: 6.0–8.1) in local herb species richness (Figure 4). Several intermediate- and fine-scale MEMs were associated with herb species richness, but residual spatial autocorrelation and normality were adequately controlled by jointly modelling random effects among plots together with MEMs. Isolation and environmental heterogeneity did not significantly explain herb species richness.

3.3.3 | Termites

Modelling termites was challenging. At the local community scale, the set of predictors tested (area, isolation and environmental heterogeneity), along with multi-scale MEMs nested within plots, explained 48% of the variation in estimated termite species richness ($R^2 = 0.477 \pm 0.068$; CI = 0.328–0.586). No ecological predictor explained the variation in the estimated termite species richness (Table 4). Removing area from the predictors did not affect the explanatory power of the BRM model (ΔLOOIC = 0.7 ± 2.7), and isolation and environmental heterogeneity also did not explain termite species richness. However, the probability of the presence of termite species modelled by a hurdle negative binomial distribution does suggest a positive effect of area increase. Accordingly, a 10% increase in area increased the probability of a *murundu* site having at least one termite species by 4.8%.

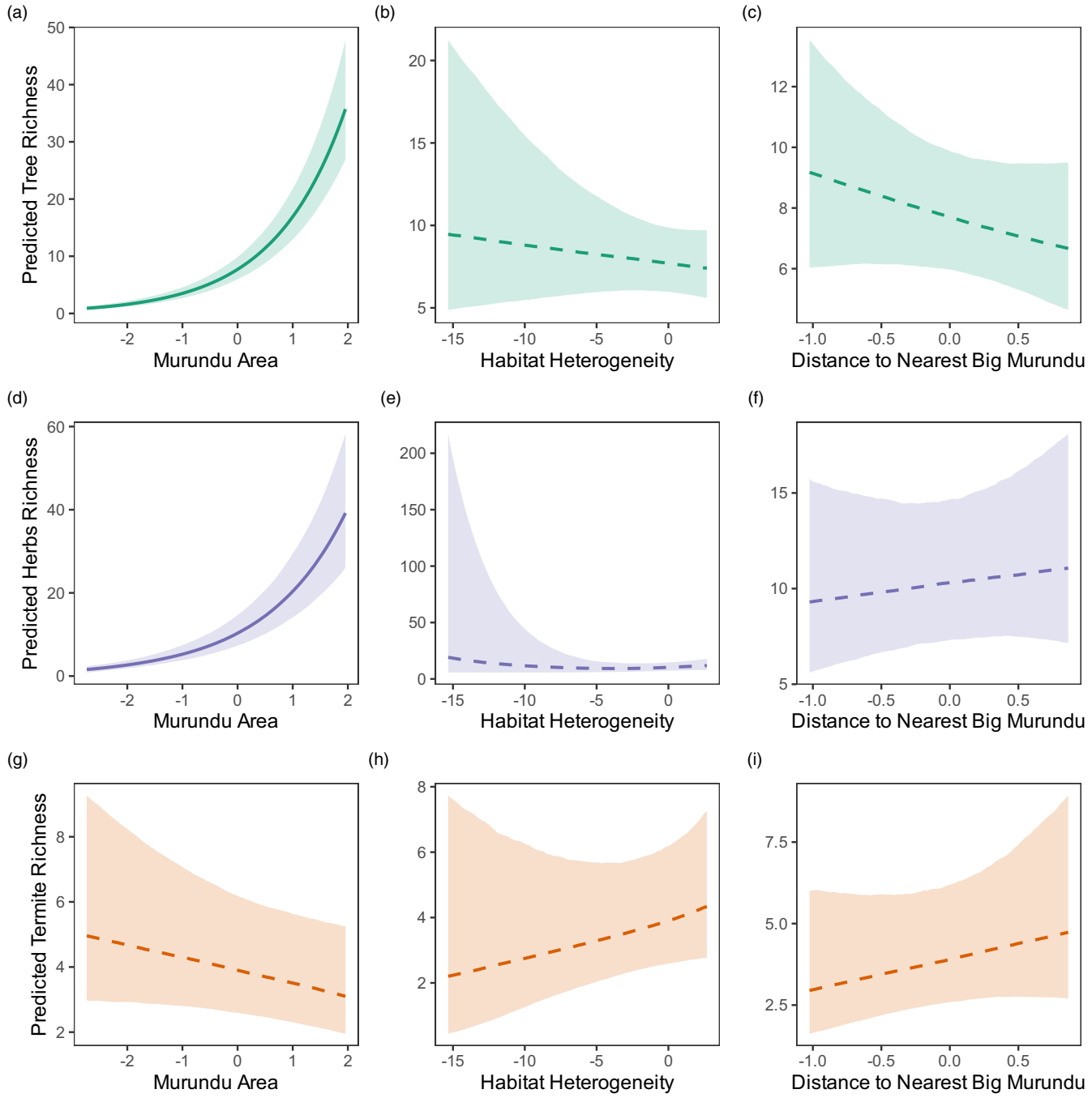

FIGURE 4 Bayesian mixed models of species richness for 11 1-ha plots in *murundu* fields sampled in Araguaia State Park, Mato Grosso, Brazil. Predicted species richness of trees as a function of *murundu* area (a), habitat heterogeneity (b) and isolation (c), and corresponding relationships for herbs (d–f) and termites (g–i). Solid lines indicate predictors with credible effects (a and d), whereas dashed lines indicate predictors without credible effects (b, c, e–i). Shaded bands represent 95% credible intervals.

Termite species richness was also associated with multiple-scale spatial filters (Table 4). Even with several MEMs to account for residual spatial autocorrelation, we could not satisfy normality assumptions via the BRM. However, the interpretation of our model for termites should be viewed with caution given several intervening factors, such as incomplete samples in some plots, non-normality of residuals as a whole and at the plot scale, and spatial autocorrelation in CM5.

A lower general explanation of the predictors for termite communities combined with greater random effects (location) indicates that different processes operate through the landscape or even that the species pool is restricted given the low dispersion capacity of termite species.

3.4 | Landscape–metacommunity patterns

There was no evidence of a direct effect of habitat amount (Figures 5a–7a) on trees, herbs and termites α-diversity. However,

TABLE 4 Results from Bayesian generalised mixed-effects mixture regression models (BRMs) for estimated termite species richness via a hurdle negative binomial distribution.

Terms	Estimate	SE	L-CI	U-CI	Rhat	Bulk_ESS	Tail_ESS
Intercept	1.10	0.30	0.51	1.68	1.00	2602	4146
shape_Intercept	−0.14	0.24	−0.64	0.30	1.00	4465	5012
hu_Intercept	−2.82	0.50	−3.83	−1.88	1.00	3680	4657
log_Area	−0.09	0.08	−0.25	0.06	1.00	5246	5020
log_Dist_Big	0.25	0.31	−0.37	0.88	1.00	5420	5426
log_Heter_veg_center	0.05	0.05	−0.03	0.17	1.00	5150	4950
MEM_PlotCM3_8	0.38	0.20	−0.04	0.78	1.00	5243	4770
MEM_PlotCM1_31	0.37	0.27	−0.16	0.91	1.00	5094	5216
MEM_PlotCM6_30	**0.98**	**0.31**	**0.42**	**1.63**	**1.00**	**4945**	**5047**
MEM_PlotCM8_46	**0.43**	**0.19**	**0.06**	**0.82**	**1.00**	**4860**	**4829**
MEM_PlotCM4_9	**0.45**	**0.18**	**0.11**	**0.81**	**1.00**	**5301**	**4971**
MEM_PlotCM8_11	−0.31	0.18	−0.67	0.04	1.00	5110	4176
MEM_PlotCM4_42	**0.40**	**0.16**	**0.10**	**0.72**	**1.00**	**4840**	**4911**
MEM_PlotCM5_27	**−0.51**	**0.23**	**−0.97**	**−0.07**	**1.00**	**4917**	**4843**
MEM_PlotCM9_1	**−0.73**	**0.32**	**−1.37**	**−0.13**	**1.00**	**5366**	**5193**
MEM_PlotCM4_6	**0.30**	**0.16**	**0.00**	**0.62**	**1.00**	**4961**	**5047**
MEM_PlotCM8_35	**0.33**	**0.16**	**0.03**	**0.64**	**1.00**	**4687**	**4890**
MEM_PlotCM4_29	**0.29**	**0.14**	**0.00**	**0.57**	**1.00**	**4764**	**4897**
MEM_PlotCM6_31	**−0.57**	**0.22**	**−1.01**	**−0.15**	**1.00**	**4691**	**4868**
MEM_PlotCM6_28	**−0.72**	**0.29**	**−1.32**	**−0.19**	**1.00**	**4632**	**5033**
MEM_PlotCM9_27	**−0.60**	**0.29**	**−1.19**	**−0.05**	**1.00**	**4702**	**4954**
MEM_PlotCM4_49	0.27	0.17	−0.07	0.61	1.00	4929	4957
MEM_PlotCM6_16	**−0.62**	**0.29**	**−1.22**	**−0.07**	**1.00**	**4997**	**5016**
shape_log_Heter_veg_center	0.02	0.11	−0.19	0.24	1.00	4708	5402
hu_log_Area	**0.49**	**0.18**	**0.16**	**0.85**	**1.00**	**5487**	**5324**
hu_log_Dist_Big	−0.78	0.63	−2.02	0.48	1.00	5391	5279
hu_log_Heter_veg_center	−0.11	0.10	−0.29	0.11	1.00	5435	5381
hu_MEM_PlotCM3_8	0.08	0.76	−1.40	1.57	1.00	4812	4709
hu_MEM_PlotCM1_31	**−0.82**	**0.39**	**−1.63**	**−0.09**	**1.00**	**5085**	**4851**
hu_MEM_PlotCM6_30	0.05	0.66	−1.23	1.39	1.00	5002	4767
hu_MEM_PlotCM8_46	0.12	0.54	−0.93	1.19	1.00	5239	4787
hu_MEM_PlotCM4_9	0.01	0.72	−1.35	1.45	1.00	5040	4706
hu_MEM_PlotCM8_11	0.42	0.53	−0.60	1.52	1.00	4598	4742
hu_MEM_PlotCM4_42	−0.05	0.70	−1.43	1.29	1.00	4939	4924
hu_MEM_PlotCM5_27	0.63	0.35	−0.02	1.35	1.00	5161	4922
hu_MEM_PlotCM9_1	**0.78**	**0.37**	**0.08**	**1.53**	**1.00**	**5121**	**4838**
hu_MEM_PlotCM4_6	−0.04	0.74	−1.47	1.44	1.00	5088	5044
hu_MEM_PlotCM8_35	0.40	0.55	−0.66	1.52	1.00	4655	4742
hu_MEM_PlotCM4_29	−0.02	0.72	−1.44	1.40	1.00	4754	4809
hu_MEM_PlotCM6_31	0.11	0.66	−1.15	1.43	1.00	5177	4998
hu_MEM_PlotCM6_28	0.06	0.66	−1.24	1.31	1.00	4876	5112
hu_MEM_PlotCM9_27	0.41	0.37	−0.28	1.14	1.00	5145	5228
hu_MEM_PlotCM4_49	0.05	0.69	−1.28	1.43	1.00	4887	4901
hu_MEM_PlotCM6_16	0.92	0.67	−0.36	2.28	1.00	4952	5241

Note: Credible predictors based on their 95% confidence intervals are shown in bold.

Abbreviations: L-CI, lower 95% confidence interval; SE, standard error; U-CI, upper 95% confidence interval.

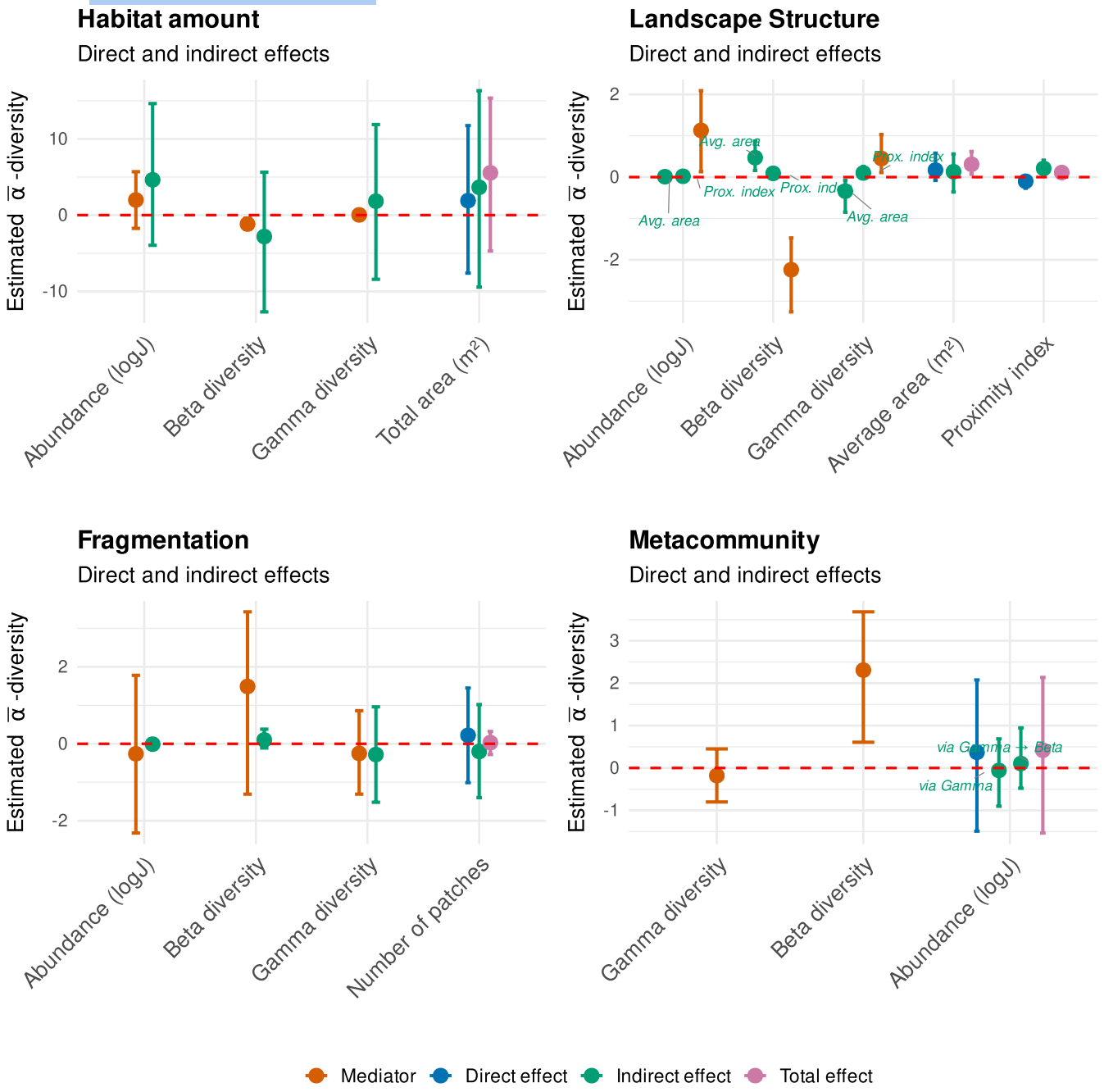

FIGURE 5 Landscape-scale effects on tree species richness for 11 1-ha plots of *murundu* fields sampled at Araguaia State Park, Mato Grosso, Brazil. The average effect sizes of the Bayesian Structural Equation Model and 95% confidence intervals are provided.

the indirect effect of landscape structure on tree α-diversity was mediated by trees total abundance (weak and positive), β-diversity (positive) and γ-diversity (negative), and these metacommunity metrics had positive, negative and positive effects, respectively. Landscape average area also had strongly positive effect on average α-diversity of herbs (Mean $\pm$ SD: 7.86 $\pm$ 3.40), specially driven by direct, indirect and mediated negative effect of β-diversity and positive effect of γ-diversity.

β-diversity indirectly and negatively affected termites α-diversity, likely because of nestedness. Residual correlations among metacommunity metrics (abundance, γ-diversity and β-diversity) direct and indirectly influence tree and herb α-diversity. Although there were no positive effects of habitat amount directly on metacommunity α-diversity, the observed effects through abundance, γ-diversity and β-diversity need more investigation, especially because our analysis relies on just 11 1-ha plots, resulting in high uncertainty and few effects, if any, besides our BSEM was able to converge with goodness-of-fit for all taxons.

Potential paths to elucidate landscape–metacommunity links should seek predictors that control the response of α-diversity, β-diversity and γ-diversity to the processes acting across multiple scales, including landscape structure. Habitat amount was not the

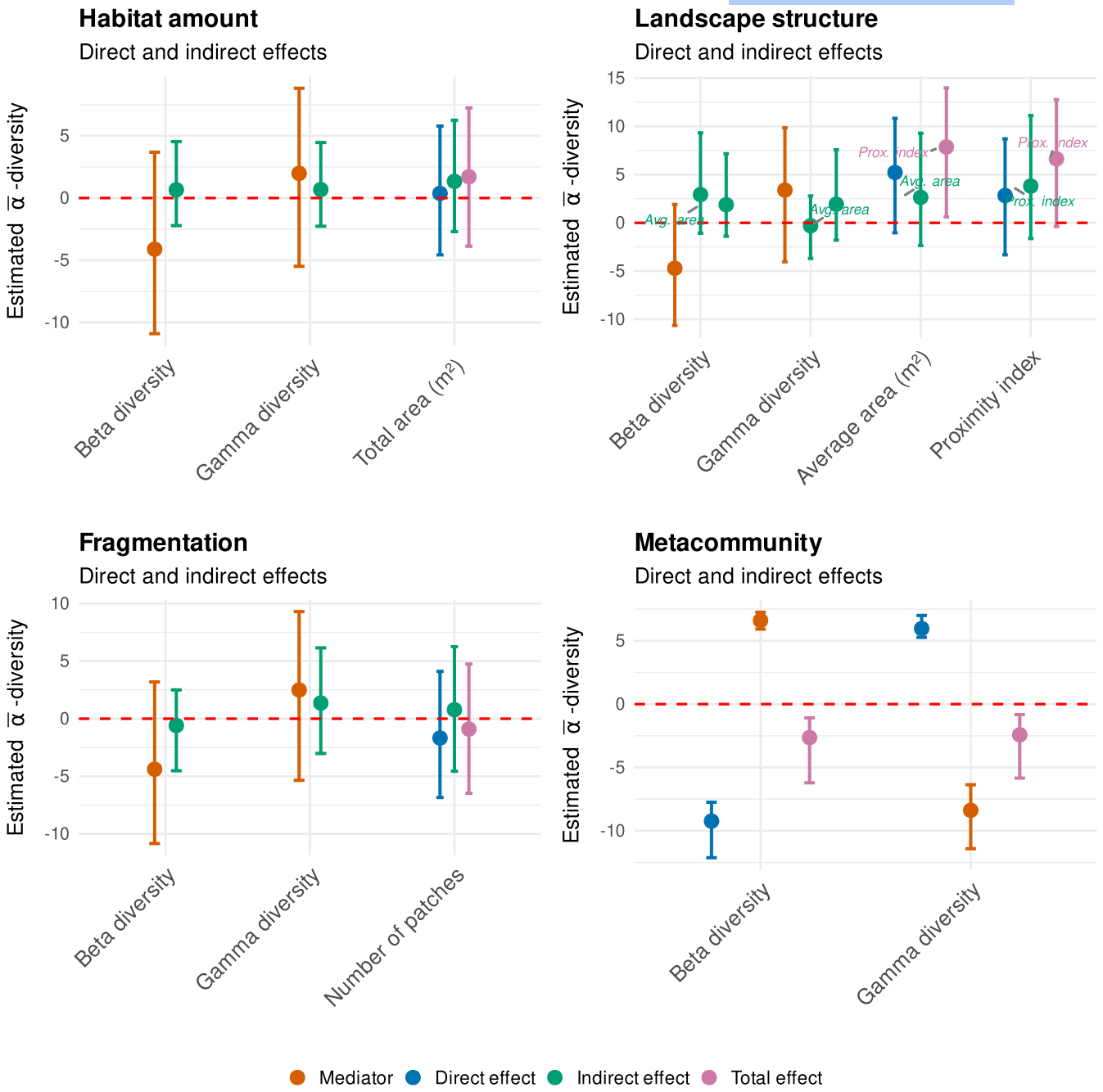

FIGURE 6 Landscape-scale effects on herb species richness for 11 1-ha plots of *murundu* fields sampled at Araguaia State Park, Mato Grosso, Brazil. The average effect sizes of Bayesian Structural Equation Model and 95% confidence intervals are provided.

only candidate mechanism driving α-diversity neither fragmentation. Moreover, the effects of landscape structure and metacommunity metrics vary among the groups likely because of dispersive constraints and other life-history traits.

4 | DISCUSSION

Overall, our results clearly show that in natural islands within South American hyperseasonal savannas, plant richness was positively related to murundu area locally, whereas at the landscape-scale habitat amount increased regional diversity and indirectly enhanced local richness, particularly for trees and herbs., whereas termite richness does not respond to any ecological, spatial or landscape processes consistently. These plant patterns largely corroborate the species–area relationships predicted by IBT (MacArthur & Wilson, 1967, 1969; Warren et al., 2015) and likely function as metacommunity connected by dispersion limitation and differential quality of bigger islands sustaining unfavourable ones, and partially corroborate Fahrig's Hypothesis (Fahrig, 2013), confirming that the amount of habitat in the landscape, rather than landscape configuration, is the key determinant of species diversity because it affects

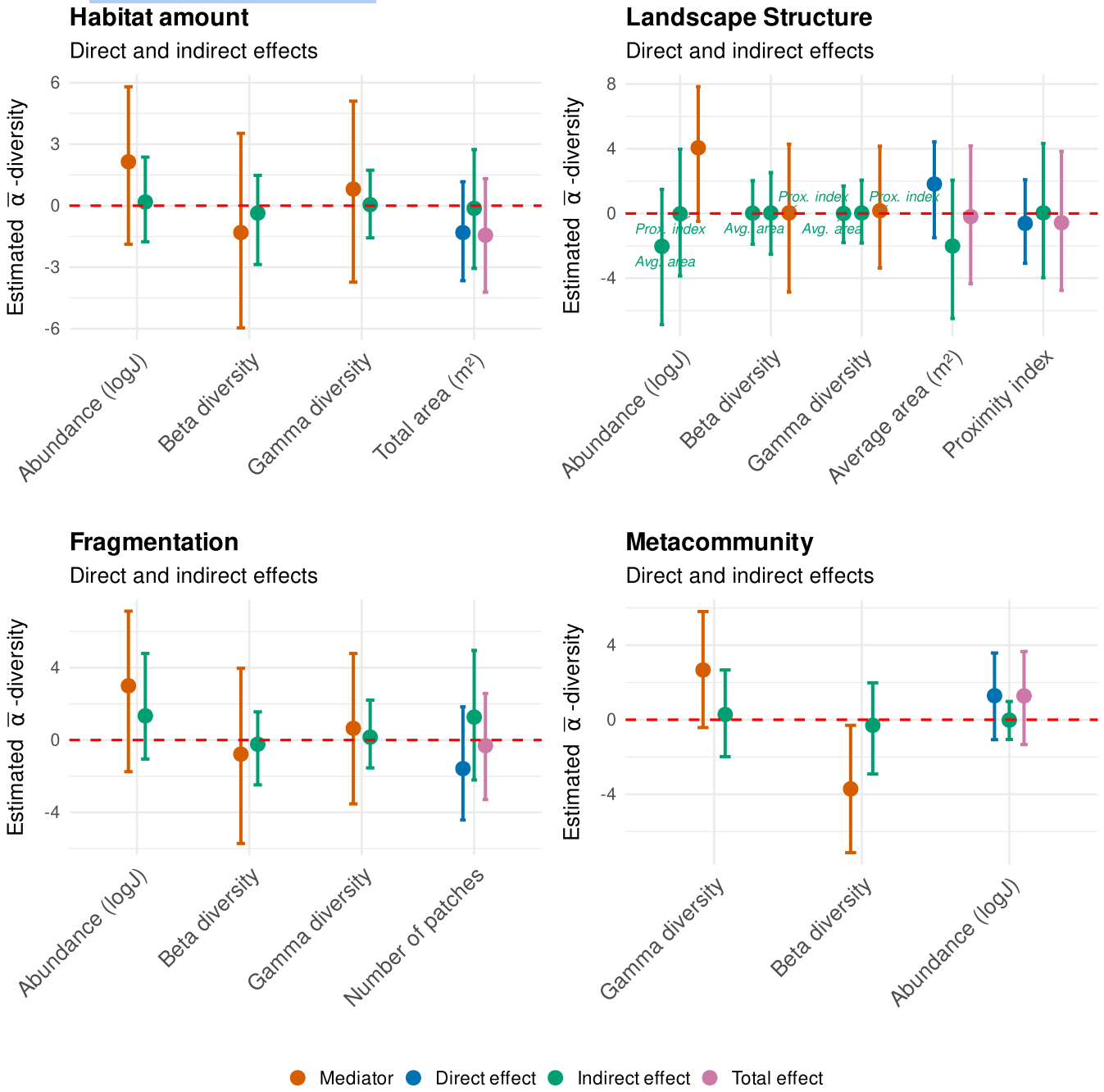

FIGURE 7 Landscape-scale effects on termite species richness in 11 1-ha plots of *murundu* fields sampled at Araguaia State Park, Mato Grosso, Brazil. The average effect sizes of Bayesian Structural Equation Model and 95% confidence intervals are provided.

metacommunity abundance, β-diversity and γ-diversity. Importantly, the lack of effect of 'fragmentation' locally here is very different from the fragmentation of forest habitat seen regionally in the 'Arc of Deforestation'. Rather, it reflects the apparent unimportance of matrix patchiness in a context where species establishment is controlled by seasonal flooding dynamics not by human activities.

For plants, species richness increased significantly with *murundu* area, partially confirming our first hypothesis (1) that tree richness is influenced by area, likely due to a lower probability of extinction, seed recruitment and sampling effects. However, there was no evidence of species-sorting along environmental heterogeneity gradients, refuting niche-based processes. Neither isolation nor environmental heterogeneity significantly affected plant or termite species richness at the local scale. The mass effects of metacommunity processes also emerge as a candidate mechanism for trees.

For herbs, species richness was also strongly and positively related to the *murundu* area, confirming our second hypothesis (2) that herbaceous species respond primarily to island size, which is consistent with mass–effect metacommunity dynamics. As with trees, isolation and local heterogeneity did not significantly affect richness, supporting the view that dispersal limitation is weak in these systems. Herbaceous species typically produce numerous, small,

wind-dispersed propagules, allowing efficient colonisation across the landscape. Consequently, area, rather than distance between islands, dictates local richness. Although environmental heterogeneity did not systematically increase herb species richness, it increased variation among *murundus*, suggesting that more heterogeneous mounds sustain more variable species assemblages even if they are not consistently richer. These results corroborate hypothesis (2) and are in line with mass–effect expectations (Leibold et al., 2004), where dispersal from larger or more productive islands maintains local diversity and nested dissimilarity is more likely to prevail over spatial turnover. At broader scales, the positive link between landscape habitat amount and regional herb richness supports the Habitat Amount Hypothesis (Fahrig, 2013), indicating that the total habitat area across the landscape, rather than the patch configuration, is the key determinant of species diversity.

These findings indicate that island size locally (not habitat heterogeneity or isolation at this scale ~1 ha), and habitat amount rather than spatial configuration at landscape scale, primarily determines vegetation diversity. The strong area effect locally may reflect both stochastic processes and increased environmental gradients favouring more environmental niches in larger *murundus*, which is consistent with passive sampling effects (Marimon et al., 2015). Positive species–area relationships have also been reported in other *murundu* fields in Central Brazil (Oliveira-Filho, 1992a, 1992b), suggesting that local area is the dominant driver of plant diversity in these mound systems and perhaps in hyperseasonal savannas more broadly.

The absence of isolation effects likely reflects effective seed dispersal across the short distances separating *murundus*, aided by wind, water and autochory. Many plant species exhibit abiotic or self-dispersal mechanisms, such as wind dispersal or explosive dehiscence, which buffer against geographic isolation (Connell, 1971; Janzen, 1970). Additional propagule input from trees in surrounding flood-prone grasslands (e.g. *Curatella americana*, *Vochysia rufa*) or nearby upland Cerrado habitats (e.g. *Caryocar brasiliense*) (Marimon et al., 2012, 2015; Marimon & Lima, 2001) further reduces the effect of isolation. Although environmental heterogeneity was present, it was unrelated to plant richness, suggesting that the ability of species to colonise contrasting microhabitats (e.g. mound summits vs. edges) compensates for local environmental variation.

The termite assemblages displayed markedly different patterns. Model performance was lower and more variable among plots, with no clear effect of area, isolation or environmental heterogeneity on species richness. Thus, hypothesis (3) was only partially supported: although termite occurrence increased slightly with area, richness itself did not. Instead, the spatial dynamics of colonisation and extinction and colony-level processes appear to dominate. The regular spatial distribution of *murundus* suggests competitive avoidance among colonies in the formation of nests, which is consistent with earlier observations of over-dispersed termite nest distribution (Bourguignon et al., 2011; Davies et al., 2016; Mathews, 1977). In fact, our analysis supports a regular spatial distribution of *murundus* throughout the landscape (Figure S3). Interspecific and intraspecific competition during colony establishment likely prevents the close co-occurrence of active nests, resulting in spatial regularity. Additionally, larger *murundus* and taller mounds may provide safer refuges from seasonal flooding, favouring the persistence of established colonies and explaining the weak positive area effect on termite presence as modelled by a *hurdle* negative binomial Bayesian mixed effect model. These results indicate that biotic interactions and colony life-history traits, rather than classical island attributes, structure termite assemblages. This outcome supports Mathews' (1977) long-standing hypothesis that colony competition and nest dynamics drive termite distribution in these ecosystems. Hence, termites are true ecosystem engineers of the *murundus* whose metacommunity dynamics exemplify non-neutral, interaction-driven assembly, which is likely governed by patch dynamics, where biotic factors outweigh area, niche-based or dispersal constraints, and seasonal flooding and fire dynamics control the success of colony establishment.

Taken together, our findings demonstrate that different ecological processes govern assemblage structure across the three groups studied. For trees and herbs, species richness depends mainly on habitat area, thus corroborating IBT predictions at local islands and the Habitat Amount Hypothesis at the landscape scale. In contrast, termite richness reflects complex biotic interactions, colony establishment dynamics and scale-dependent spatial structuring, partially supporting the hypothesis (iv) that plants depend more on the total habitat amount and area, whereas termites depend more on colonisation-extinction trade-offs, as expected under patch dynamics (Leibold et al., 2004).

The *murundu* fields therefore represent a natural model system for testing and integrating classical local and contemporary landscape–metacommunity theories. They reveal how species–area relationships, mass effects, biotic interactions and colonisation–extinction mechanisms (e.g. patch dynamics) interact to shape biodiversity across spatial scales. Future studies combining long-term field monitoring and remote-sensing approaches could clarify the temporal dynamics of mound formation, colony turnover and plant colonisation, enhancing the understanding of these unique Neotropical Island ecosystems. Predicting species–area relationships and the rate of species turnover (β-diversity) due to island size—and the relative contribution of turnover and nestedness—may also provide the rules needed to accurately predict landscape-level γ-diversity. Finally, the work helps illustrate not only the natural uniqueness of the *campos de murundus* ecosystem, but also its contribution to ecological science as a model system for testing ecological theory. Our hope is that these values can help strengthen conservation strategies and action in the ASP, which is facing external threats to the viability *of murundus*.

AUTHOR CONTRIBUTIONS

Henrique A. Mews and Denis S. Nogueira developed the questions, analysed the data and wrote the first draft. Beatriz S. Marimon proposed the experimental design, approved the financing and developed the questions. Henrique A. Mews and Beatriz S. Marimon collected the field data. Reginaldo Constantino contributed to the

design of the termite sampling protocol and identified the termite specimens. All authors contributed critically to the drafts and gave final approval for publication.

ACKNOWLEDGEMENTS

We thank the editor and the anonymous reviewers for their thorough, constructive and useful comments on earlier versions of this manuscript, which significantly improved the quality of the study. We thank Herson S. Lima, Halina S. Jancoski, Daniel D. Franczak and Micheli C. Moresco, who participated in the fieldwork. The Article Processing Charge for the publication of this research was funded by the Coordenação de Aperfeiçoamento de Pessoal de Nível Superior - Brasil (CAPES) (ROR identifier: 00x0ma614).

FUNDING INFORMATION

The study was supported by the Foundation for Research Support of the state of Mato Grosso (FAPEMAT; Proc. 97/04), the Program of Academic Agreement/Coordination for the Improvement of Higher-Level Education (PROCAD/CAPES; Proc. 109/2007) and the Brazilian National Council for Scientific and Technological Development (CNPq)—Special Visiting Researcher (CNPq/PVE; Proc. 401279/2014-6). B.S. Marimon and B.H. Marimon-Junior were supported by the CNPq/Bolsa Produtividade em Pesquisa (301153/2018-3, 303492/2022-8 and 311027/2019-9) and O. L. Phillips was supported by an ERC Advanced Grant and a Royal Society Wolfson Research Merit Award.

CONFLICT OF INTEREST STATEMENT

The authors declare no conflicts of interest.

PEER REVIEW

The peer review history for this article is available at https://www.webofscience.com/api/gateway/wos/peer-review/10.1111/1365-2745.70305.

DATA AVAILABILITY STATEMENT

The vouchers of the termite specimens collected are in the permanent insect collection of the Department of Zoology, University of Brasília, Brasília, Brazil, and the vouchers of all the plant species are in the NX Herbarium, State University of Mato Grosso, Nova Xavantina, Mato Grosso, Brazil. The complete list of plant species is provided in Marimon et al. (2012, 2015) https://doi.org/10.1590/S0102-33062012000100018 and https://doi.org/10.1086/682079, respectively. Data and code used in statistical analyses are available from the Dryad Digital Repository: https://doi.org/10.5061/dryad.612jm64kr (Mews et al., 2026).

ORCID

Henrique A. Mews https://orcid.org/0000-0002-7489-8197
Denis S. Nogueira https://orcid.org/0000-0001-8893-7903
Ben Hur Marimon-Junior https://orcid.org/0000-0002-6359-6281
Reginaldo Constantino https://orcid.org/0000-0003-2060-6723
Oliver L. Phillips https://orcid.org/0000-0002-8993-6168
Beatriz S. Marimon https://orcid.org/0000-0003-3105-2914

REFERENCES

Akaike, H. (1974). A new look at the statistical model identification. *IEEE Transactions on Automatic Control*, *19*, 716–723.

Allouche, O., Kalyuzhny, M., Moreno-Rueda, G., Pizarro, M., & Kadmon, R. (2012). Area-heterogeneity tradeoff and the diversity of ecological communities. *Proceedings of the National Academy of Sciences of the United States of America*, *109*(43), 17495–17500. https://doi.org/10.1073/pnas.1208652109

Anderson, M. J. (2001). A new method for non-parametric multivariate analysis of variance. *Austral Ecology*, *26*(1), 32–46. https://doi.org/10.1111/j.1442-9993.2001.01070.pp.x

Anderson, M. J., Ellingsen, K. E., & McArdle, B. H. (2006). Multivariate dispersion as a measure of beta diversity. *Ecology Letters*, *9*(6), 683–693. https://doi.org/10.1111/j.1461-0248.2006.00926.x

Arrhenius, O. (1921). Species and area. *Journal of Ecology*, *9*, 95–99. https://doi.org/10.2307/2255763

Baddeley, A., Rubak, E., & Turner, R. (2015). *Spatial point patterns: Methodology and applications with R*. Chapman and Hall/CRC Press.

Bartoń, K. (2018). *MuMIn*: *Multi-model inference* (R package version 1.42.1). https://CRAN.R-project.org/package=MuMIn

Batalha, M. A., Cianciaruso, M. V., Silva, I., & Delitti, W. B. (2005). Hyperseasonal cerrado, a new Brazilian vegetation form. *Brazilian Journal of Biology*, *65*, 735–738. https://doi.org/10.1590/s1519-69842005000400021

Bates, D., Mächler, M., Bolker, B., & Walker, S. (2015). Fitting linear mixed-effects models using lme4. *Journal of Statistical Software*, *67*(1), 1–48. https://doi.org/10.18637/jss.v067.i01

Bauman, D., Drouet, T., Dray, S., & Vleminckx, J. (2018). Disentangling good from bad practices in the selection of spatial or phylogenetic eigenvectors. *Ecography*, *41*(10), 1638–1649. https://doi.org/10.1111/ecog.03380

Bauman, D., Fortin, M.-J., Drouet, T., & Dray, S. (2018). Optimizing the choice of a spatial weighting matrix in eigenvector-based methods. *Ecology*, *99*(10), 2159–2166. https://doi.org/10.1002/ecy.2469

Bender, D. J., & Fahrig, L. (2005). Matrix structure obscures the relationship between interpatch movement and patch size and isolation. *Ecology*, *86*(4), 1023–1033. https://doi.org/10.1890/03-0769

Besag, J. (1977). Some methods of statistical analysis for spatial data. *Bulletin of the International Statistical Institute*, *47*, 77–92.

BFG. (2015). Growing knowledge: An overview of seed plant diversity in Brazil. *Rodriguésia*, *66*(4), 1085–1113. https://doi.org/10.1590/2175-7860201566411

Blanchet, F. G., Legendre, P., & Borcard, D. (2008). Forward selection of explanatory variables. *Ecology*, *89*(9), 2623–2632. https://doi.org/10.1890/07-0986.1

Bourguignon, T., Leponce, M., & Roisin, Y. (2011). Are the spatio-temporal dynamics of soil-feeding termite colonies shaped by intra-specific competition? *Ecological Entomology*, *36*(6), 776–785. https://doi.org/10.1111/j.1365-2311.2011.01328.x

Brooks, M. E., Kristensen, K., van Benthem, K. J., Magnusson, A., Berg, C. W., Nielsen, A., Skaug, H. J., Maechler, M., & Bolker, B. M. (2017). glmmTMB balances speed and flexibility among packages for zero-inflated generalized linear mixed modelling. *The R Journal*, *9*, 378–400. https://doi.org/10.32614/RJ-2017-066

Brunsdon, C., & Comber, A. (2019). *An introduction to R for spatial analysis and mapping* (2nd ed.). SAGE Publications.

Bürkner, P.-C. (2017). Brms: An R package for Bayesian multilevel models using Stan. *Journal of Statistical Software*, *80*(1), 1–28. https://doi.org/10.18637/jss.v080.i01

Bürkner, P.-C. (2018). Advanced Bayesian multilevel modelling with the R package brms. *The R Journal*, *10*(1), 395–411. https://doi.org/10.32614/RJ-2018-017

Bürkner, P.-C. (2021). Bayesian item-response modelling in R with brms and Stan. *Journal of Statistical Software*, *100*(5), 1–54. https://doi.org/10.18637/jss.v100.i05

Burnham, K. P., & Anderson, D. R. (2002). *Model selection and multimodel inference: A practical information-theoretic approach* (2nd ed.). Springer. https://doi.org/10.1007/b97636

Chao, A., Gotelli, N. J., Hsieh, T. C., Sander, E. L., Ma, K. H., Colwell, R. K., & Ellison, A. M. (2014). Rarefaction and extrapolation with hill numbers: A framework for sampling and estimation in species diversity studies. *Ecological Monographs*, *84*, 45–67. https://doi.org/10.1890/13-0133.1

Chao, A., & Jost, L. (2012). Coverage-based rarefaction and extrapolation: Standardizing samples by completeness rather than size. *Ecology*, *93*(12), 2533–2547. https://doi.org/10.1890/11-1952.1

Colwell, R. K., Chao, A., Gotelli, N. J., Lin, S.-Y., Mao, C. X., Chazdon, R. L., & Longino, J. T. (2012). Models and estimators linking individual-based and sample-based rarefaction, extrapolation and comparison of assemblages. *Journal of Plant Ecology*, *5*, 3–21. https://doi.org/10.1093/jpe/rtr044

Connell, J. H. (1971). On the role of natural enemies in preventing competitive exclusion in some marine animals and in rain forest trees. In P. J. Boer & G. R. Gradwell (Eds.), *Dynamics of populations* (pp. 298–312). Centre for Agricultural Publishing and Documentation.

Connor, E. F., & McCoy, E. D. (1979). The statistics and biology of the species-area relationship. *The American Naturalist*, *113*(6), 791–833.

Cressie, N. A. C. (1991). *Statistics for spatial data*. John Wiley & Sons.

Davies, A. B., Baldeck, C. A., & Asner, G. P. (2016). Termite mounds alter the spatial distribution of African savanna tree species. *Journal of Biogeography*, *43*(2), 301–313. https://doi.org/10.1111/jbi.12633

Dengler, J. (2009). Which function describes the species–area relationship best? A review and empirical evaluation. *Journal of Biogeography*, *36*(5), 728–744. https://doi.org/10.1111/j.1365-2699.2008.02038.x

Diggle, P. J. (1986). Parametric and non-parametric estimation for pairwise interaction point processes. In Proc. 1st World Congr. Bernoulli Society.

Diniz-Filho, J. A. F., Rangel, T. F. L. V., & Bini, L. M. (2008). Model selection and information theory in geographical ecology. *Global Ecology and Biogeography*, *17*(4), 479–488. https://doi.org/10.1111/j.1466-8238.2008.00395.x

Dray, S., Bauman, D., Blanchet, G., Borcard, D., Clappe, S., Guenard, G., Jombart, T., Larocque, G., Legendre, P., Madi, N., Wagner, H. H., & Siberchicot, A. (2023). adespatial: Multivariate multiscale spatial analysis. *R package version 0.3-28*. https://doi.org/10.32614/CRAN.package.adespatial

Dray, S., Legendre, P., & Peres-Neto, P. R. (2006). Spatial modelling: A comprehensive framework for principal coordinate analysis of neighbour matrices (PCNM). *Ecological Modelling*, *196*(3–4), 483–493. https://doi.org/10.1016/j.ecolmodel.2006.02.015

Fahrig, L. (2003). Effects of habitat fragmentation on biodiversity. *Annual Review of Ecology, Evolution, and Systematics*, *34*, 487–515. https://doi.org/10.1146/annurev.ecolsys.34.011802.132419

Fahrig, L. (2013). Rethinking patch size and isolation effects: The habitat amount hypothesis. *Journal of Biogeography*, *40*(9), 1649–1663. https://doi.org/10.1111/jbi.12130

Furley, P. A. (1986). Classification and distribution of murundus in the Cerrado of Central Brazil. *Journal of Biogeography*, *13*(3), 265–268. https://doi.org/10.2307/2844925

Hortal, J., Triantis, K. A., Meiri, S., Thébault, E., & Sfenthourakis, S. (2009). Island species richness increases with habitat diversity. *The American Naturalist*, *174*(6), E205–E217. https://doi.org/10.1086/645085

Hsieh, T. C., Ma, K. H., & Chao, A. (2018). *iNEXT: iNterpolation and EXTrapolation for species diversity*. R Packag. version 2.0.15. https://CRAN.R-project.org/package=iNEXT

Hubbell, S. P. (2001). *The unified neutral theory of biodiversity and biogeography*. Princeton University Press.

Hutchinson, G. E. (1957). Concluding remarks. *Cold Spring Harbor Symposia on Quantitative Biology*, *22*, 415–427. https://doi.org/10.1101/SQB.1957.022.01.039

Janzen, D. H. (1970). Herbivores and the number of tree species in tropical forests. *The American Naturalist*, *104*(940), 501–528. https://doi.org/10.1086/282687

Kadmon, R., & Allouche, O. (2007). Integrating the effects of area, isolation, and habitat heterogeneity on species diversity: A unification of Island biogeography and niche theory. *The American Naturalist*, *170*(3), 443–454. https://doi.org/10.1086/519853

Leibold, M. A., Holyoak, M., Mouquet, N., Amarasekare, P., Chase, J. M., Hoopes, M. F., Holt, R. D., Shurin, J. B., Law, R., Tilman, D., Loreau, M., & Gonzalez, A. (2004). The metacommunity concept: A framework for multi-scale community ecology. *Ecology Letters*, *7*(7), 601–613. https://doi.org/10.1111/j.1461-0248.2004.00608.x

Lomolino, M. V., & Weiser, M. D. (2001). Towards a more general species–area relationship: Diversity on all islands, great and small. *Journal of Biogeography*, *28*(6), 431–445. https://doi.org/10.1046/j.1365-2699.2001.00550.x

Loosmore, N. B., & Ford, E. D. (2006). Statistical inference using the G or K point-pattern spatial statistics. *Ecology*, *87*, 1925–1931. https://doi.org/10.1890/0012-9658(2006)87[1925:SIUTGO]2.0.CO;2

Lüdecke, D., Ben-Shachar, M. S., Patil, I., Waggoner, P., & Makowski, D. (2021). Performance: An R package for assessment, comparison and testing of statistical models. *The Journal of Open Source Software*, *6*(60), 3139. https://doi.org/10.21105/joss.03139

MacArthur, R. H., & Wilson, E. O. (1967). *The theory of Island biogeography*. Princeton University Press.

MacArthur, R. H., & Wilson, E. O. (1969). Experimental zoogeography of islands: The colonization of empty islands. *Ecology*, *50*(2), 278–296. https://doi.org/10.2307/1934856

Marimon, B. S., Colli, G. R., Marimon-Junior, B. H., Mews, H. A., Eisenlohr, P. V., Feldpausch, T. R., & Phillips, O. L. (2015). Ecology of floodplain campos de murundus savanna in southern Amazonia. *International Journal of Plant Sciences*, *176*(7), 670–681. https://doi.org/10.1086/682079

Marimon, B. S., & Lima, E. S. (2001). Caracterização fitofisionômica e levantamento florístico preliminar no Pantanal dos Rios Mortes-Araguaia, Cocalinho, Mato Grosso, Brasil. *Acta Botânica Brasílica*, *15*(2), 213–229. https://doi.org/10.1590/S0102-33062001000200008

Marimon, B. S., Marimon-Junior, B. H., Lima, H. S., Jancoski, H. S., Franczak, D. D., Mews, H. A., & Moresco, M. C. (2008). *Pantanal do Araguaia-ambiente e povo: guia de ecoturismo*. Editora UNEMAT.

Marimon, B. S., Marimon-Junior, B. H., Mews, H. A., Jancoski, H. S., Franczak, D. D., Lima, H. S., Lenza, E., Rossette, A. N., & Moresco, M. C. (2012). Florística dos campos de murundus do Pantanal do Araguaia, Mato Grosso, Brasil. *Acta Botânica Brasílica*, *26*(1), 181–196. https://doi.org/10.1590/S0102-33062012000100018

Martini, P. R. (2006). Áreas úmidas da América do Sul registradas em imagens de satélites. In J. S. V. Silva & M. M. Abdon (Eds.), *Anais do 1º Simpósio de Geotecnologias no Pantanal* (pp. 876–882). Embrapa Informática Agropecuária/INPE.

Mathews, A. G. A. (1977). *Studies on termites from the Mato Grosso state, Brazil*. Academia Brasileira de Ciências.

McGillycuddy, M., Warton, D. I., Popovic, G., & Bolker, B. M. (2025). Parsimoniously fitting large multivariate random effects in glmmTMB. *Journal of Statistical Software*, *112*, 1–19. https://doi.org/10.18637/jss.v112.i01

Mews, H. A., Nogueira, D. S., Marimon-Junior, B. H., Constantino, R., Phillips, O. L., & Marimon, B. S. (2026). Data and code from: Unravelling the drivers of island species richness in tropical savannas. *Dryad Digital Repository*. https://doi.org/10.5061/dryad.612jm64kr

Mittermeier, R. A., Gil, P. R., Hoffmann, M., & Pilgrim, J. (2005). *Hotspots revisited: Earth's biologically richest and most endangered ecoregions*. Conservation International.

Nakagawa, S., & Schielzeth, H. (2013). A general and simple method for obtaining R^2 from generalized linear mixed-effects models. *Methods in Ecology and Evolution*, *4*(2), 133–142. https://doi.org/10.1111/j.2041-210X.2012.00261.x

Oksanen, J., Blanchet, F. G., Friendly, M., Kindt, R., Legendre, P., McGlinn, D., Minchin, P. R., O'Hara, R. B., Simpson, G. L., Solymos, P., Stevens, M. H. H., Szoecs, E., & Wagner, H. (2018). Vegan: Community ecology package. R package version 2.5–2. https://CRAN.R-project.org/package=vegan

Oliveira-Filho, A. T. (1992a). Floodplain "murundus" of Central Brazil: Evidence for the termite-origin hypothesis. *Journal of Tropical Ecology*, *8*(1), 1–19. https://doi.org/10.1017/S0266467400006027

Oliveira-Filho, A. T. (1992b). The vegetation of Brazilian "murundus"- the Island-effect on the plant community. *Journal of Tropical Ecology*, *8*(4), 465–486. https://doi.org/10.1017/S0266467400006817

Ponce, V. M., & Cunha, C. N. (1993). Vegetated earthmounds in tropical savannas of Central Brazil: A synthesis: With special reference to the Pantanal do Mato Grosso. *Journal of Biogeography*, *20*(2), 219–225. https://doi.org/10.2307/2845673

Presley, S. J., & Willig, M. R. (2022). From Island biogeography to landscape and metacommunity ecology: A macroecological perspective of bat communities. *Annals of the New York Academy of Sciences*, *1514*(1), 43–61. https://doi.org/10.1111/nyas.14785

R Core Team. (2025). *R: A language and environment for statistical computing*. R Foundation for Statistical Computing. https://www.R-project.org

Ratter, J. A., Bridgewater, S., & Ribeiro, J. F. (2003). Analysis of the floristic composition of the Brazilian Cerrado vegetation. III: Comparison of the woody vegetation of 376 areas. *Edinburgh Journal of Botany*, *60*(1), 57–109. https://doi.org/10.1017/S0960428603000064

Ribeiro, J. F., & Walter, B. M. T. (2008). As Principais Fitofisionomias do Bioma Cerrado. In S. M. Sano, S. P. Almeida, & J. F. Ribeiro (Eds.), *Cerrado: ecologia e flora* (pp. 151–212). Embrapa Informação Tecnológica.

Ricketts, T. H. (2001). The matrix matters: Effective isolation in fragmented landscapes. *The American Naturalist*, *158*(1), 87–99. https://doi.org/10.1086/320863

Ripley, B. D. (1977). Modelling spatial patterns. *Journal of the Royal Statistical Society. Series B, Statistical Methodology*, *39*, 172–212. https://doi.org/10.1111/j.2517-6161.1977.tb01615.x

Sarmiento, G. (1984). *The ecology of neotropical savannas*. Harvard University.

Schloerke, B., Cook, D., Larmarange, J., Briatte, F., Marbach, M., Thoen, E., Elberg, A., & Crowley, J. (2025). *GGally: Extension to 'ggplot2'*. (R package version 2.4.0). https://CRAN.R-project.org/package=GGally

Silva, L. C. R., Vale, G. D., Haidar, R. F., & Sternberg, L. S. L. (2010). Deciphering earth mound origins in central Brazil. *Plant and Soil*, *336*(1–2), 3–14. https://doi.org/10.1007/s11104-010-0329-y

Stan Development Team. (2023). *RStan: the R interface to Stan*. R package version 2.32.7. https://mc-stan.org/

Warren, B. H., Simberloff, D., Ricklefs, R. E., Aguilée, R., Condamine, F. L., Gravel, D., Morlon, H., Mouquet, N., Rosindell, J., Casquet, J., Conti, E., Cornuault, J., Pellissier, L., & Mazel, F. (2015). Islands as model systems in ecology and evolution: Prospects fifty years after MacArthur–Wilson. *Ecology Letters*, *18*, 200–217. https://doi.org/10.1111/ele.12398

Whittaker, R. H. (1960). Vegetation of the Siskiyou Mountains, Oregon and California. *Ecological Monographs*, *30*(3), 279–338. https://doi.org/10.2307/1943563

SUPPORTING INFORMATION

Additional supporting information can be found online in the Supporting Information section at the end of this article.

Figure S1. Satellite images of *campos de murundus* (earth-mound fields) in Araguaia State Park, Mato Grosso, Brazil, taken at altitudes of 2000 m (a) and 700 m (b), and a ground-level photograph (c). Satellite images source: Google Earth®; ground-level photograph by B. H. Marimon-Junior.

Figure S2. Density estimation of the occurrence and spatial distribution of *murundus* in 11 1-ha plots of *campo de murundus* (CM; earth-mound fields) sampled in Araguaia State Park, Mato Grosso, Brazil. Higher concentrations of *murundus* are indicated by multiple closed density-contour circles.

Figure S3. Analysis of both observed and expected spatial distribution patterns, based on Ripley's *K*-function, for 11 1-ha plots of *campo de murundus* (CM; earth-mound fields) sampled in Araguaia State Park, Mato Grosso, Brazil. Observed values of Ripley's *K* are shown as a solid black line, whereas theoretical expectations are shown in red.

Figure S4. Descriptive analysis of environmental predictors of variation in species richness of trees, herbs and termites in 11 1-ha plots of *campo de murundus* (earth-mound fields) sampled at Araguaia State Park, Mato Grosso State, Brazil. Histograms along the diagonals show absolute values of *murundu* area (m^2) and height (m), distance between *murundus* (m), number of termite nests per *murundu* and environmental heterogeneity for plants and termites. Scatter plots in the lower left zone show relationships between environmental predictors, with best-fit splines, with the equivalent linear correlations (Pearson's *r*) displayed in the top right zone.

Figure S5. Habitat heterogeneity, defined for plants based on *murundu* height and volume, and for termites based on the number of nests, both quantified as the distance to the centroid of 11 1-ha plots derived from the 'betadisper' function with Euclidean distance.

Figure S6. Metacommunity abundance density and asymptotic species richness density distribution for 373 *murundus* islands within 11 1-ha plots. For all taxonomic groups the shape of the density distribution follows a known left-skewed pattern of abundance and species counts, whereas the magnitude of rare species concentration varies among taxonomic groups.

Figure S7. Evaluation of BRM model predictions and simulated tree species richness at plot scale for the metacommunity features. Landscape-scale BRM model assumptions are not shown due to the absence of credible effects.

Figure S8. Evaluation of BRM model predictions and simulated herb species richness at plot scale for the metacommunity features. Landscape-scale BRM model assumptions are not shown due to the absence of credible effects.

Figure S9. Evaluation of BRM model predictions and simulated termite species richness at plot scale for the metacommunity features. Landscape-scale BRM model assumptions are not shown due to the absence of credible effects.

Figure S10. DHARMa residual analysis of the BRM model for estimated tree species richness and overall model performance. (A) Posterior predictive checks indicate that hurdle negative binomial distribution adequately captures the overall pattern of species richness. (B) Residuals were uniformly distributed according to the

Kolmogorov–Smirnov test ($D = 0.064$, $p = 0.091$), with no evidence of overdispersion (dispersion = 0.713, $p = 0.174$) or outliers ($p = 1.000$), confirming that the BRM model provides a good fit to the data and yields credible estimates.

Figure S11. DHARMa residual analysis of the BRM model for estimated herb species richness and overall model performance. (A) Posterior predictive checks indicate that the hurdle negative binomial distribution adequately captures the overall pattern of species richness. (B) Residuals were uniformly distributed according to the Kolmogorov–Smirnov test ($D = 0.570$, $p = 0.614$), with no evidence of outliers (p-value = 0.840) and only slight overdispersion (dispersion = 0.506, $p = 0.044$), confirming that the BRM model provides a good fit to the data and yields credible estimates.

Figure S12. DHARMa residual analysis of the BRM model for estimated termite species richness showed the following results: (A) Posterior predictive checks indicate that the hurdle negative binomial distribution provides a good fit to the data, and (B) some deviation from normality according to the Kolmogorov–Smirnov test ($D = 0.150$, $p < 0.0001$), insignificant overdispersion (dispersion = 0.300, $p = 0.104$), and no evidence of outliers ($p = 0.240$). Despite the slight non-normality observed in the residuals of the BRM fitted with a hurdle negative binomial distribution, we chose to interpret the results because they were consistent with those obtained from the GAM model fitted with a smooth spline for area and likely reflect local species extinctions in small *murundu* islands (Table S4).

Table S1. Diggle–Cressie–Loosmore–Ford (DCLF) test of complete spatial randomness (CSR) within 11 1-ha plots. Significance of the summary statistic L(r) was tested using a Monte Carlo test based on 999 simulations.

Table S2. DHARMa Moran's *I* test of spatial autocorrelation in the residuals of the BRM model estimating tree species richness across *murundu* plots. For each plot, as well as for the aggregated dataset, the DHARMa Moran's *I* test did not detect distance-based autocorrelation (observed = −0.124, expected = −0.100, SD = 0.087, $p = 0.776$).

Table S3. DHARMa Moran's *I* test of spatial autocorrelation in the residuals of the BRM model estimating herb species richness across *murundu* plots. For the aggregated plots, the DHARMa Moran's *I* test did not detect distance-based autocorrelation (observed = −0.144, expected = −0.100, SD = 0.088, p-value = 0.618), although significant spatial autocorrelation was detected in the residuals for plot CM7 and CM9.

Table S4. DHARMa Moran's *I* test of spatial autocorrelation in the residuals of the BRM model estimating termite species richness across *murundu* plots. For the aggregated plots, the DHARMa Moran's *I* test did not detect distance-based autocorrelation (observed = −0.1999, expected = −0.100, SD = 0.088, $p = 0.263$), although significant spatial autocorrelation was detected in the model residuals for plot CM5.

Table S5. Shrub and tree species and their abundances, along with seed dispersal modes, sampled in 11 1-ha plots of *campo de murundus* (earth-mound fields) in Araguaia State Park, Mato Grosso, Brazil. The complete plant species list is available in Marimon et al. (2012, 2015).

Table S6. Average effect sizes from the Bayesian Structural Equation Model for landscape-scale tree species richness, with corresponding standard deviations and 2.5% and 97.5% credible intervals. Values shown in bold indicate statistically significant effects.

Table S7. Average effect sizes from the Bayesian Structural Equation Model for landscape-scale herb species richness, with corresponding standard deviations and 2.5% and 97.5% credible intervals. Values shown in bold indicate statistically significant effects.

Table S8. Average effect sizes from the Bayesian Structural Equation Model for landscape-scale termite species richness, with corresponding standard deviations and 2.5% and 97.5% credible intervals. Values shown in bold indicate statistically significant effects.

How to cite this article: Mews, H. A., Nogueira, D. S., Marimon-Junior, B. H., Constantino, R., Phillips, O. L., & Marimon, B. S. (2026). Unravelling the drivers of island species richness in tropical savannas. *Journal of Ecology*, *114*, e70305. https://doi.org/10.1111/1365-2745.70305